Authors response to Referee n° 1

We are thankful for the constructive and helpful comments that have helped us to improve our manuscript. We are aware that the manuscript holds a high amount of data which can be difficult to follow at some points and tried to keep it as concise as possible. We considered all comments carefully and modified and followed most of the suggestions.

Specific Comments from Referee n° 1

2) The introduction reads well. One question is whether you have a testable hypothesis. Are you trying to ask whether the corals are fueled by fluids versus scavenging from currents. How are you going to distinguish between mechanisms?

Response: the aim of the study is to address the linkage between CWCs and present day formation of MDACs in the Pompeia Province. For this purpose, we combined analyses of ROV images, geophysical data and sample materials. For instance, we analyzed $\delta^{13}C$ signatures of coral skeletons to evaluate whether these organisms were directly relying on CH_4. We found that the coral skeletons exhibited significantly higher $\delta^{13}C$ values than the co-occurring AOM-derived carbonates, thus not supporting CH_4 as important carbon source. Rather, the corals were feeding on material suspended in currents.

3) In the methods please add section in which you describe the Experimental Design. How many samples were collected and from where? The descriptions of the laboratory methods are okay. However, I have no idea if you sampled thoroughly enough.

Response: we included more detailed information on our sample strategy and study design in the material and methods section.

4) In Table 2, will readers know what Identifier means? I realize that the numbers correspond to pictures in the figures. However, it is very confusing to have to put the figure next to the table to interpret the data in the table. There must be a better way to present the data.

Response: done. We replaced "Identifier" by "Identification number in Fig. 7". In Addition, we added an additional column to the table in which we provide information on the analyzed material.

5) Rather than using code numbers for the sampling sites, it would help readers if you used descriptive names, such as 'active seep', etc.

Response: done. We have revised the use of code numbers throughout the manuscript.

6) Although amplicon sampling for microbial group is okay. Do you have evidence for microbial growth and activity? Perhaps in the discussion indicate which samples come from fresh material and are likely to have fresh DNA versus samples in which the DNA could be old and preserved. I realized this is inferred by looking at the pictures, but again this is a convoluted way to present a story.

Response: we have improved the information concerning the DNA material related to each sample in the manuscript, and we have specified the type of sample from which the DNA has been extracted (lines 183–186 in the revised manuscript). Furthermore, we added some extra information in Fig. 11 to clarify and

remain the type of sample. DNA analyses cannot conclude if DNA is “old” or “fresh”, but we can estimate (together with other analyses) if the sample used for this analysis is fresh or not. but we can infer this by assessing the relative age and preservation of the analyzed sample. For instance, an AOM-derived carbonate recovered from an active pockmark (sample D10-R7) exhibits more DNA of AOM-related microorganisms (ANME and SRB) than oxidized AOM-derived carbonates recovered from regions that are currently not affected by seepage (sample D10-R3).

7) I suppose the model is okay. However, again a better presentation of the data might lead readers to the conclusion rather than relying on the author’s story.
Response: done. We have modified the last paragraph of the section 4.3. for a better understanding of our model (lines 439–446 in the revised manuscript).

Technical Comments from Referee n° 1
1) Line 19: consider saying, ‘rate a seepage via focused, scattered, diffused, etc.’
Response: done. We revised the sentence to “the type of seepage such as focused, scattered, diffused or eruptive”.

2) Line 34: change ‘which’ to ‘that’.
Response: done.

3) Line 36: change to ‘typically, they thrive, etc.’
Response: done.

4) Line 45: change ‘ecological’ to ‘environmental’ and ‘are discussed to control’ to ‘influence’.
Response: done.

5) Line 51: delete ‘e.g.’.
Response: done.

6) Line 53: change ‘e.g.’ to ‘for example’.
Response: done.

7) Line 65: delete ‘i.e.’ and the parentheses. The text is not an example rather it is the description of ‘coral graveyards.’
Response: done.

Authors response to Referee n° 2

We are thankful for your constructive feedback and the helpful comments. We have considered and addressed your suggestions carefully, and almost all have been followed in the revised manuscript.

Detail Comments from Referee n° 2

1) Line 1. Title. The text after the hyphen: 'living on the edge' is unnecessary and adds nothing to the title. What edge? I suggest removing this.

Response: we would like to keep the text "living on the edge" to emphasize that hydrocarbon-rich seepage has both advantages and disadvantages for cold-water corals growth.

2) Lines 26-27. Abstract Delta C13 values of the coral skeletons (see below)

Response: see discussion on reviewer comment nº 19 below.

3) Line 31. Abstract. Suggest 'seeping' rather than 'seeped' fluids.

Response: done.

4) Line 61. Suggest 'In addition' to replace 'On the other hand', as this is not a contrasting observation.

Response: done.

5) Line 76. 'Englobes' is not an English word. Seems like a transliteration of 'encompasses'.

Response: done.

6) Line 128. Don't start sentence with a number – spell it out.

Response: done.

7) Line 152. Can the authors give a little more detail of the nature of the samples used for the DNA work. Are these MDACs?

Response: done. We now provide more information on the nature of the samples (lines 182–185 in the revised manuscript).

8)Lines 192-195. The background information about the Gulf of Cadiz isn't really results and would go better at the start of section 2.

Response: we agree that the background information of the Gulf of Cádiz is not part of results. However, the Pompeia Province region, which our study is focused on, has not been described in detail so far. We here provide the first description of geological structures in this area (Southern and Northern Pompeia Coral ridges, Cold-water Coral Mounds Fields), including novel data (e.g., bathymetry, seismics). For this reason, we consider it appropriate to report these findings in the results sections.

9) Line 241 and other places. It's quite difficult at the moment to correlate the isotopic

data in Table 2 with the sample points in Figure 7, because the specimen images in Figure 7 are not quite large enough to distinguish samples of authigenic carbonates from embedded coral skeletons. Therefore, could the authors add a column into Table 2 that makes it clear what the samples are for each of the isotopic data points, e.g. authigenic carbonate or coral skeleton.

Response: done. One more column has been added in Table 2 as proposed, indicating the type of samples from which stable isotopic analyses are.

10) Line 253. Replace 'stems' with 'comes'.

Response: done.

11) Line 254. In the figure the 'worms' look like serpulid worm tubes. Is this so? In which case please add this information.

Response: done.

12) Line 291. Replace 'On the contrary' with 'In contrast'.

Response: done.

13) Line 296. Spell out '2D' at start of sentence.

Response: done.

14) Line 305 and elsewhere. What is 'dripping-like' seepage? This isn't a description I recognize, so it would be helpful if the authors specify what this means.

Response: done. "Dripping-like refers to intermittent bubbling fluids" (lines 343–344 in the revised manuscript).

15) Line 317. Suggest 'data', rather than 'evidences'.

Response: done.

16) Line 330. I'm unclear where is being referred to here.

Response: removed.

17) Line 332. 'appear', not 'appears', as preceding diapirs is plural.

Response: done.

18) Line 339. Typo. Angle not angel.

Response: done.

19) Lines 346-354. The authors here suggest that the seawater-like values of the delta C13 from the dead scleractinian skeletons and those embedded in the MDAC show that the corals do not use

methane as a food source, either directly or through symbionts. The authors need to be careful here, because some seep organisms that demonstrably do use methane (and sulfide) from seep fluids for food via endosymbionts produce carbonate skeletons that also have seawater-like delta C13 signatures. I am referring here to vesicomyid and bathymodiolin bivalves, that sequester seawater bi-carbonate ions to produce their shells. Using this model, having seawater-like delta C13 values in the coral skeletons does not prove that these animals do not use chemosynthetic food sources at the site. Really, to be able to settle this conclusively, authors would have to do isotopic, histological and DNA work on living corals from their site, not just on skeletal material and MDAC. In addition, it would be worth noting that scleractinian corals are found embedded in ancient seep carbonates too (see Goedert and Peckmann 2005); there may be some useful comparative isotopic data in that paper.

Response: We included the paper by Goedert and Peckmann, 2005. We fully agree that analyses of coral tissues ($\delta^{13}C$, DNA) would add important information on their nutrition and metabolic relationships. However, we still regard $\delta^{13}C$ values of their skeletons as valuable proxy for the possible uptake of CH_4. Corals utilize HCO_3^- deriving from both the environment and the internal production of CO_2 for skeleton biomineralization (Swart, 1983; Zoccola et al., 2015; Nakamura et al., 2018). Therefore, if they uptake CH_4 as a carbon source, the CO_2 produced from CH_4 metabolism would be used, and consequently parts of the HCO_3^- utilized for biomineralization would be isotopically depleted. This "mixing effect" would result in at least partially depleted $\delta^{13}C$ values of the skeletons, similar to some chemosynthetic vesicomyid and lucinid bivalves (Hein et al., 2006). The skeletons of the corals analyzed herein, however, exhibit significantly higher $\delta^{13}C$ values than the co-occurring AOM-derived carbonates. Thus, they are not indicative for CH_4 as important carbon source.

20) Lines 364-367. The entombment of coral skeletons by MDAC may have no consequence to corals, if they are already dead. It's not entirely clear from the text if the corals associated with the MDAC are dead or alive. If they are alive then this argument is stronger. Also, in most seep environments MDACs form in the subsurface where AOM reactions are occurring. Is this the case at this site? What proof is there of active MDAC formation at the sediment-water interface, as indicated in Figure 12? This is pertinent to the arguments in section 4.3.

Response: We cannot determine if the scleractinian corals embedded in AOM-derived carbonates (samples D10-R3 and D11-R8) were alive or dead when they were buried (lines 812-813 in the revised manuscript). However, we observed living corals in areas that are currently affected by seepage (e.g. the Northern Pompeia Coral Ridge, lines 262–263 in the revised manuscript; Fig. 6, C). Furthermore, we observed living octocorals growing on surfaces of currently formed AOM-derived carbonates (e.g., in an active pockmark in the Al Gacel MV, sample D10-R7; Fig. 5, C). These observations imply that corals in these regions are directly affected by methane seepage and the microbially mediated formation of carbonates due to AOM.

References

Hein, J. R., Normark, W. R., McIntyre, B. R., Lorenson, T. D., and Powell, C. L.: Methanogenic calcite, 13C-depleted bivalve shells, and gas hydrate from a mud volcano offshore southern California, Geology, 34(2), 109–112, 2006.

Nakamura, T., Nadaoka, K., Watanabe, A., Yamamoto, T., Miyajima, T., and Blanco, A. C.: Reef-scale modeling of coral calcification responses to ocean acidification and sea-level rise, Coral Reefs, 37, 2018.

Swart, P. K.: Carbon and Oxygen Isotope Fractionation in ScleracUnian Corals: a Review, Earth-Sci. Rev., 19, 51–80, 1983.

Zoccola, D. Ganot, P., Bertucci, A., Caminit-Segonds, N., Techer, N., Voolstra, C. R., Aranda, M., Tambutté, E., Allemand, D., Casey, J. R., and Tambutté, S.: Bicarbonate transporters in corals point towards a key step in the evolution of cnidarian calcification, Sci. rep.-UK, 5, 2015.

Authors response to Referee n° 3

We are thankful for your useful and interesting comments. We hope we have addressed successfully the different issues discussed here.

Main issues

-The authors write that the "This study aims at elucidating the linkage between the present-day formation of MDACs and CWCs development along the Pompeia Province (Fig. 1),", but it is not clear why the selected analysis is the best way to achieve this. For example, "Petrographic analysis" is described in the Methods but it is not clear why this analysis is necessary to answer the questions addressed in the manuscript. The suspected nutritional linkage between CWC and hydrocarbon seepage is known in the literature as the 'hydraulic theory' (see Hovland, Jensen et al. 2012 and references therein). The present study is a direct test of this theory in an area that is very suited to test this. The name "hydraulic theory" and/or related reference are however not mentioned in the manuscript (e.g. ln 50-52)

Response: The "hydraulic theory" is now included in the introduction with references (line 55 of revised manuscript). Petrographic analyses are needed to be sure that these are seep carbonates, and to find the right sampling points for isotope analysis — we have to discriminate between authigenic carbonates, corals, micritic phases. of samples. For instance, embedded corals in some of the AOM-carbonates (D10-R3 and D11-R8) have been described and discriminated from the AOM-carbonate facies by petrographic analysis.

-Another major problem was description of the sampling design and the method of sampling. The authors write on line 84-86 "This study is based on collected data from the Pompeia Province, during the Subvent-2 cruise in 2014 aboard the R/V Sarmiento de Gamboa. The analysed samples were recovered from the Al Gacel MV (D10-R3, D10-R7, D11-R8) and the Northern Pompeia Coral Ridge (D03-B1) (Fig. 1)." This description is grossly inadequate. What was the sampling design? Are 'samples' collected ad random or based a preconceived plan? Why those sites? What material was sampled as 'the samples' (e.g. living coral pieces, coral rubble, sediment with rubble, carbonates)? Size/weight of the samples? Number of samples? Replication? How are the samples taken (ROV arm, push core)? How were samples stored on the ROV, how long before samples reached the surface how are samples processed/stored on-board (significant given the DNA/RNA analysis, e.g. with respect to cross contamination, microbial community shifts)?

Detailed response to "*What was the sampling design? Are 'samples' collected ad random or based a preconceived plan? Why those sites? How are the samples taken (ROV arm, push core)? How were samples stored on the ROV, how long before samples reached the surface how are samples processed/stored on-board (significant given the DNA/RNA analysis, e.g. with respect to cross contamination, microbial community shifts)?*: we included more information on the study design, storage and sampling procedure in the material and methods section (see lines 91–102 on the new revised manuscript). We also added a new table (Table 1) with detailed information of the sampling material.

Detailed response to *"What material was sampled as 'the samples' (e.g. living coral pieces, coral rubble, sediment with rubble, carbonates)? Size/weight of the samples? Number of samples? Replication?"*: Information about the samples (what is each sample) is detailed in the "Petrography and stable isotopes of carbonates" results (section 3.3). Size of the samples are given with a scale bar in Fig. 7 (A, C, E, F). Weight of the samples was not determined. Each sample is one unit (i. e. coral fragment, carbonate from the based of the Al Gacel MV, carbonate from an active pockmark in Al Gacel MV, and carbonate from the summit of the Al Gacel MV). Replicates used for DNA analysis have been described in section 2.6.1. Furthermore, stable isotopic values obtained from precise sampling sites performed on each sample (section 2.4) are shown in Figure 7 (B, D, F) and Table 3.

The authors are addressing ecological questions (see e.g. line 34-38, line 50-52 and line 75 "…present-day formation of MDACs and CWCs development…") using studies of carbonates. One of the issues that is particularly relevant for the interpretation of these data is whether the analysis was performed on carbonates with living CWC or not. From the pictures and description, it seems plausible that only dead CWC carbonates were studied (although ln 348 mentions "the necrotic part of living *Madrepora*"), but this begs the question how representative the RNA/DNA/biomarker analysis is when only carbonates of dead CWCs are studied. To what extent do the authors think that the organic components of the carbonates still represent the CWC microbial community? Similarly for the 13C carbonate analysis, is it known well enough whether CWCs leave a distinct isotope mark in the carbonates that is representative for feeding on surface derived organic matter versus hydrocarbons? Targeted sampling of also living CWC pieces and comparison with the sampled carbonates would have provided a means to address this.

Response: since the necrotic coral-carbonate (D03-B1) used for environmental DNA analysis belongs to a living *Madrepora oculata* (see line 303), it is expected that 16S rDNA libraries reveal DNA related to microorganisms related to the corals' microbiota. For instance, sequences related to Enterobacteria and Verrucomicrobia were found in this sample (Supplementary **Table S1**) and are normally in the environment and found associated with corals and other animals (Sorokin et al., 1995; Webster et al., 2016), while *Nitrosococcus* bacteria are ammonia-oxidizers, probably involved in the regulation of nitrogen cycle of the coral's holobiont (Rädecker et al., 2015). Thus, we would have found DNA related to chemosynthetic microorganisms in case the coral fed from the seeping fluids.

Furthermore, it has been supported by many that coral-carbonate skeletons do partially reflect corals nutrition, since part of the $HCO3^-$ used for its formation comes from the coral's metabolism, i. e. CO_2 formed from cellular respiration (Swart, 1983; Zoccola et al., 2015; Nakamura et al., 2018) (lines 392–397 from the revised manuscript). Thus, stable carbon isotopic analysis is an optimal procedure to observe if corals used methane as a carbon source.

-The authors mention that the ROV had sensors for CO2 and CH4 data and could take NISKIN water samples for CH4. In the results section (ln 219-221 and ln 231) CH4 data are mentioned but in the M&M nothing can be found on sampling location (e.g. height above sediment), sensor calibration, samples handling, sample analyses of the water samples.

Response: Pore-water analysis (from micro-cores) as well as seawater analysis (from Niskin bottles) have been included in this manuscript (see section 2.2.1). However, CH_4 measurements have not been included in the material and methods section since those measurements have been done by colleagues from the Subevent-2 project which have previously published the methane values recovered from the Niskin bottles. Sampling procedure can be found in their publication (Sánchez-Guillamón et al., 2015).

The site description in 3.1 should be partly moved to the Materials and Methods. Only the new results from this study should stay in 3.1.

Response: the Pompeia Province region has been described in detail for the first time in this study. We provide geological structures in this area (Southern and Northern Pompeia Coral ridges, Cold-water Coral Mounds Fields), including novel data (e.g., bathymetry, seismics). Therefore, we consider it appropriate to report these findings in the results sections.

-The authors infer that "severe seepage results in lethal conditions for CWCs" (line 363 - 364 and 377-378), but I see no evidence for that in the paper. In addition, the authors concluded that CWCs can be entombed by MDAC formation, it is however not clear whether this entombment is the cause of CWC mortality or that this entombment took place after CWC demise following for example from post-glacial decrease in current strength.

Response: We cannot determine if the scleractinian corals embedded in AOM-derived carbonates (samples D10-R3 and D11-R8) were alive or dead when they were buried (lines 812–813 from revised manuscript). However, we observed living corals in areas that are currently affected by seepage (e.g. the Northern Pompeia Coral Ridge, lines 264–265 in the revised manuscript; Fig. 6, C). Furthermore, we observed living octocorals growing on surfaces of currently formed AOM-derived carbonates (e.g., in an active pockmark in the Al Gacel MV, sample D10-R7; Fig. 5, C). These observations indicate that CWCs can live when seepage occurs by means of the "buffer effect" (section 4.3) but severe seepage which cannot be completely buffered may end killing the CWCs.

Suggestions for minor edits:

-ln 48-50: reduce number of refs

Response: done.

-ln 59: reduce number of refs

Response: done.

-ln 72-73: reduce number of refs

Response: done.

-ln 112: Please also give the values of the VPDB used, to avoid confusion

Response: done. Please see lines 140–142 of the new revised manuscript.

-ln 124: "have a global distribution" instead of "globally widespread"
Response: done in line 21 of the revised manuscript.

-ln 152: replace "… solid samples were…" with "…sample material was…"
Response: done.

-ln 230: replace "…by dead.." with "… by shells of the chemosynthetic bivalves Lucinoma…"
Response: done.

-ln 243: What does "virtually influenced" mean?
Response: "virtually" was deleted.

-ln 262: "… values ranging from…". From the methods it is unclear on what this range is based, replication, multiple samples?
Response: The range is based on the different values obtained along the same petrographic facies of each sample (Figs. 7 & 9; Table 2). The numbers shown on the petrographic sections of each sample in Figure 7 (Fig. 7, B, D, F), indicate the exact sampling points used for stable isotopic analysis, which values are shown in Table 2. Further information has been included in the foot of Fig. 7 to facilitate this information for the readers.

-ln 307: What does "proportions" here mean? Do you mean "rates" or "concentrations"?
Response: concentrations. Changed.

-ln 308: So was methane sampled upon removal of the carbonate blocks?
Response: yes. Information added in line 352 of the new revised manuscript (see Sánchez-Guillamón et al., 2015 for details).

-ln 368: The authors also mentioned the availability of a CO2 sensor on the ROV. Has this been used to measure aragonite saturation states at the different locations?
Response: Because of the lack of exact data (xcf. Sánchez-Guillamón et al., 2015), aragonite saturation was not calculated. Interestingly, Niskin samples revealed high fCO2 in Al Gacel MV above the seafloor (Sánchez-Guillamón et al., 2015), which may have an effect on the CWC, though experiments showed acclimation of *Lophelia* to changing aragonite saturation (Form et al., 2012). More accurate measurements would have been needed to approach the aragonite saturation state of the different locations.

-ln 755: Fig 4C. There is a black pointing to "octocorals", but I cannot see these on the picture.
Response: they are on top of the carbonate, difficult to observed since they are semi-transparent. Figure was improved.

References

Form, A. U, and Riebesell, U.: Acclimation to ocean acidification during long-term CO2 exposure in the cold-water coral *Lophelia pertusa*, Global Change Biology. 18, 843–853, 2012.

Nakamura, T., Nadaoka, K., Watanabe, A., Yamamoto, T., Miyajima, T., and Blanco, A. C.: Reef-scale modeling of coral calcification responses to ocean acidification and sea-level rise, Coral Reefs, 37, 2018.

Rädecker, N., Pogoreutz, C., Voolstra, C. R., Wiedenmann, J., and Wild, C: Nitrogen cycling in corals: The key to understanding holobiont functioning?, Trends Microbiol., 23(8), 490–497, 2015.

Sánchez-Guillamón, O., García, M. C., Moya-Ruiz, F., Vázquez, J. T., Palomino, D., Fernández-Puga, M. C., and Sierra, A.: A preliminary characterization of greenhouse gas (CH4 and CO2) emissions from Gulf of Cádiz mud volcanoes, VIII Symposium MIA15, 2015.

Sorokin, Y. I.: Coral reef ecology. Vol. 102, Springer Science & Business Media, 1995.

Swart, P. K.: Carbon and Oxygen Isotope Fractionation in ScleracUnian Corals: a Review, Earth-Sci. Rev., 19, 51–80, 1983.

Webster, N. S., Negri, A. P., Botté, E. S., Laffy, P. W., Flores, F., Noonan, S., ... and Uthicke, S.: Host-associated coral reef microbes respond to the cumulative pressures of ocean warming and ocean acidification, Scientific reports, 6, 19324, 2016.

Zoccola, D. Ganot, P., Bertucci, A., Caminit-Segonds, N., Techer, N., Voolstra, C. R., Aranda, M., Tambutté, E., Allemand, D., Casey, J. R., and Tambutté, S.: Bicarbonate transporters in corals point towards a key step in the evolution of cnidarian calcification, Sci. rep.-UK, 5, 2015.

Authors response to Editor

Dear Dr Rincón-Tomás

Thank you for submitting your revised manuscript. I would like to request some additional changes, many of which aim to ensure that the reasoning you provide in response to reviewer comments is actually included in the manuscript discussion. Please could you therefore undertake further revisions to accommodate the comments below.

Best regards,

Clare Woulds

Authors: we appreciate your constructive comments on our manuscript. We are also thankful for the extra time you have given us to improve the manuscript and address successfully all discussion points.

You mention twice that the aim of the study was to '...address the linkage between CWCs and present day formation of MDACs.' The fact that two reviewers have questioned the study objectives / hypotheses supports my feeling that the phrase 'address the linkage' is not sufficiently explicit. Please re-phrase your aim and research questions in plainer language, and state the hypothesis that you were testing.
Response: we have now modified the last paragraph of the introduction (lines 80–89 of the revised manuscript), in which we present our hypothesis and clarify the aim of our study.

Please ensure that the answer to reviewer 2 point 19 is included in the discussion, with appropriate acknowledgement that the tissue you analysed was not living biomass (i.e. coral polyps), that analysis of such live tissue would be required to draw firm conclusions that methane C was not a major dietary C source, and stressing that the conclusion that can be drawn is that methane C was not a major C source during building of the exoskeleton. I recognise your point that if the corals were using methane derived C, then when it was metabolised some of it may be incorporated into the exoskeleton. However, the lack of (much) evidence for this is a rather tenuous way of drawing a conclusion about how the corals fulfilled their metabolic needs.
Response: We have added more information addressing this issue in the discussion, between lines 391–394 and 409 from the revised manuscript. We specify our analyzed sample is a "necrotic part of a living *Madrepora oculata*" in line 396.

Likewise, please include the response to reviewer 2 point 2o in the discussion.
Response: Response to reviewer 2, point 20 has been included. In the results section we specify the observation of living corals along the Northern Pompeia Coral Ridge (lines 262–264 of revised manuscript; Fig. 6), as well as the presence of living octocorals on top of a currently formed MDAC (line 260 of revised

manuscript; Fig. 5). We have also added an aclaration on the foot of Figure 6 (lines 812–813), in which we indicate that we cannot determine if the corals were alive when buried. We have considered that this information is better adapted to those sections, rather than in the discussion section.

Please ensure that all responses to reviewer 3 are also included in the text.
Response: done.

Line 53 – 'Supports' should be replaced with 'suggests'.
Response: done.

Please add a table, referred to in the opening paragraphs of the method section (therefore Table1), detailing study site lat and long, depths, and number of samples of each type collected. Please also indicate the number of replicate samples of each type collected at each location.
Response: A table (now Table 1) has been added to remark and clarify the sampling sites, as well as the type of samples recovered from those sites. Since those samples were unique, there are no replicates of the original samples. Some analysis (e. g. stable isotopes, environmental DNA) do use different replicates from the same sample in order to accomplish stronger results, and those methods can be found in the material and methods section.

Please add identification of internal and external standards used for GC and isotopic analyses, as well as indications of precision for quantification of lipids and isotopic ratios.
Response: in case of stable isotopic analyses of the carbonates, accuracy and reproducibility were checked through the replicate analysis of a standard (NBS19), and the reproducibility was better than 0.1 ‰. This information is already provided in the methods section.
In case of stable carbon isotopic analyses of organic compounds, CO_2 of known stable carbon isotopic composition was used for internal calibration. This information is already provided in the methods section. The reference CO_2 was calibrated with a standard (IAEA600). Standard deviations of duplicate sample measurements were better than 1.0 ‰. We included this information into the method section.
Lipid biomarkers were not quantified, therefore no standard was needed.

Line 413-end of discussion. Your hypothesis regarding a biological buffer requires further discussion and possibly evidence. The two questions that occur to me are: 1) Is the presence of sulphide and methane normally prohibitive to the existence of CWCs? At what concentrations do they become problematic? Sulphide is of course toxic at certain concentrations, but non-chemosynthetic 'normal' or 'background' benthic fauna can and do inhabit sites with some level of sulphide flux (see Bell et al. 2016, Frontiers in Marine Science), and methane is even less of a problem. 2) Do you have evidence (i.e. porewater and bottom water methane and S- concentrations) to show that bacterial activity does indeed lead to reductions in sulphide concentrations such that they allow colonisation by CWCs? I'd suggest that there is another explanation, which is that CWCs are tolerant to some extent of sulphide

and methane fluxes, however sulphide and methane may cause some degree of stress, which may at least partially explain the poor health (low abundance of living material) that you observed.

Detail response to "*1) Is the presence of sulphide and methane normally prohibitive to the existence of CWCs? At what concentrations do they become problematic? Sulphide is of course toxic at certain concentrations, but non-chemosynthetic 'normal' or 'background' benthic fauna can and do inhabit sites with some level of sulphide flux (see Bell et al. 2016, Frontiers in Marine Science), and methane is even less of a problem":* We agree that non-chemosynthetic fauna is able to live in conditions where sulfide and methane fluxes are present in "some level". Interestingly, when seepage of methane and/or sulfide occurs, there is normally chemosynthetic-fauna related to this seepage, which are actually "buffering" the harmful "levels" that could affect those non-chemosynthetic fauna if they would not feed on the seeped fluids. As we observed in Fig. 12, A, which represents the active pockmark found in the Al Gacel MV (Fig. 5), CWCs are living in an active pockmark and actually colonizing a currently-formed AOM carbonate. Furthermore, methane is indeed not toxic for CWCs, but its emission decreases pH and complicates carbonate precipitation (which affects CWCs like scleractinians).

Detailed response to *"2) Do you have evidence (i.e. porewater and bottom water methane and S-concentrations) to show that bacterial activity does indeed lead to reductions in sulphide concentrations such that they allow colonisation by CWCs? I'd suggest that there is another explanation, which is that CWCs are tolerant to some extent of sulphide and methane fluxes, however sulphide and methane may cause some degree of stress, which may at least partially explain the poor health (low abundance of living material) that you observed"*: we have now included S- and Fe values obtained from pore-water and seawater samples (see section 2.2.1 and lines 269 – 275 of new revised manuscript). S- and Fe values in the pore-water are higher that those from the bottom seawater, which indicates its consumption. This can be explained by the observation of framboidal pyrite inside the carbonate D10-R7 (Fig. 8 C–D), as well as environmental bacterial DNA sequences which indicate the presence of sulfide-oxidizing bacteria. Furthermore, ROV images also indicate the presence of siboglinid worms that also consume this sulfide.

Authors additional modifications

1) Line 3: Francisco Javier González instead of Javier González.

2) Lines 4 and 10: Names and information related to new co-authors, Esther Santofimia and Enrique López-Pamo.

3) Line 35: “such as Siboglinidae worms” added.

4) Line 59: “in northern Rockall Trough”.

5) Line 70: “with only a few living corals”.

6) Line 118: new section including water analysis.

7) Lines 268–275: water parameters improved.

8) Lines 360–361: water analysis results included in discussion

Cold-water corals and hydrocarbon-rich seepage in the Pompeia Province (Gulf of Cádiz) — living on the edge

Blanca Rincón-Tomás[1], Jan-Peter Duda[2,3], Luis Somoza[43], Francisco Javier González[43], Dominik Schneider[1], Teresa Medialdea[43], Esther Santofimia[54], Enrique López-Pamo[54], Pedro Madureira[565], Michael Hoppert[1], and Joachim Reitner[26,73]

[1]Georg-August-University Göttingen, Institute of Microbiology and Genetics, Grisebachstraße 8, 37077 Göttingen, Germany
[2]Department of Earth Sciences, University of California Riverside, CA 92521, USA
[2]Georg-August-University Göttingen, Göttingen Centre of Geosciences, Goldschmidtstraße 3, 37077 Göttingen, Germany
[3]Göttingen Academy of Sciences and Humanities, Theaterstraße 7, 37073 Göttingen, Germany
[34]Marine Geology Dept., Geological Survey of Spain, IGME, Ríos Rosas 23, 28003 Madrid, Spain
[45]Geological Resources Dept., Geological Survey of Spain, IGME, Ríos Rosas 23, 28003 Madrid, Spain
[565]Estrutura de Missão para a Extensão da Plataforma Continental (EMEPC). Rua Costa Pinto 165, 2770-047 Paço de Arcos, Portugal
[62]Georg-August-University Göttingen, Göttingen Centre of Geosciences, Goldschmidtstraße 3, 37077 Göttingen, Germany
[7]
[73]Göttingen Academy of Sciences and Humanities, Theaterstraße 7, 37073 Göttingen, Germany

Correspondence to: Blanca Rincón-Tomás (b.rincontomas@gmail.com)

Abstract. Azooxanthellate cold-water corals (CWCs) have a global distribution and have commonly been found in areas of active fluid seepage. The relationship between the CWCs and these fluids, however, is not well understood. This study aims at unraveling the relationship between CWC development and hydrocarbon-rich seepage in the Pompeia Province (Gulf of Cádiz, Atlantic Ocean). This region comprises mud volcanoes, coral ridges and fields of coral mounds, which are all affected by the tectonically driven seepage of hydrocarbon-rich fluids. The type of seepage such as focused, scattered, diffused or eruptive, however, is tightly controlled by a complex system of faults and diapirs. Early diagenetic carbonates from the currently active Al Gacel MV exhibit δ^{13}C-signatures down to −28.77 ‰ VPDB, indicating biologically derived methane as the main carbon source. The same samples contained ^{13}C-depleted lipid biomarkers diagnostic for archaea such as crocetane (δ^{13}C down to −101.2 ‰ VPDB) and PMI (δ^{13}C down to −102.9 ‰ VPDB), evidencing microbially mediated anaerobic oxidation of methane (AOM). This is further supported by next generation DNA sequencing data, demonstrating the presence of AOM related microorganisms (ANME archaea, sulfate-reducing bacteria) in the carbonate. Embedded corals in some of the carbonates and CWC fragments exhibit less negative δ^{13}C values (−8.08 to −1.39‰ VPDB), pointing against the use of methane as the carbon source. Likewise, the absence of DNA from methane- and sulfide-oxidizing microbes in a sampled coral does not support a chemosynthetic lifestyle of these organisms. In the light of these findings, it appears that the CWCs benefit rather indirectly from hydrocarbon-rich seepage by using methane-derived authigenic carbonates as a substratum for colonization. At the same time, chemosynthetic organisms at active sites, such as Siboglinidae worms, prevent coral dissolution and necrosis by feeding on the seeping fluids (i. e. methane, sulfate, hydrogen sulfide), allowing cold-water corals to colonize carbonates currently affected by hydrocarbon-rich seepage.

Con formato: Superíndice
Con formato: Superíndice
Con formato: Superíndice
Con formato: Inglés (Estados Unidos)
Con formato: Superíndice
Con formato: No agregar espacio entre párrafos del mismo estilo, Ajustar espacio entre texto latino y asiático, Ajustar espacio entre texto asiático y números
Con formato: Inglés (Estados Unidos)
Con formato: Superíndice
Con formato: Sin Resaltar
Con formato: Superíndice
Con formato: Inglés (Estados Unidos)

1. Introduction

Cold-water corals (CWCs) are a widespread, non-phylogenetic group of cnidarians that include hard skeleton scleractinian corals, soft-tissue octocorals, gold corals, black corals and hydrocorals (Roberts et al., 2006; Roberts et al., 2009; Cordes et al., 2016). Typically, they thrive at low temperatures (4 – 12 ºC) and occur in water depths of ca. 50 – 4000 m. CWCs are azooxanthellate and solely rely on their nutrition as energy and carbon sources (Roberts et al., 2009). Some scleractinian corals (e.g. *Lophelia pertusa*, *Madrepora oculata*, *Dendrophyllia cornigera*, *Dendrophyllia alternata*, *Eguchipsammia cornucopia*) are able to form colonies or even large carbonate mounds (Rogers et al., 1999; Wienberg et al., 2009; Watling et al., 2011; Somoza et al., 2014). Large vertical mounds and elongated ridges formed by episodic growth of scleractinian corals (mainly *Lophelia pertusa*) are for instance widely distributed along the continental margins of the Atlantic Ocean (Roberts et al., 2009). These systems are of great ecological value since they offer sites for resting-, breeding-, and feeding for various invertebrates and fishes (Cordes et al., 2016 and references therein).

Several environmental forces influence the initial settling, growth, and decline of CWCs. These include, among others, an availability of suitable substrates for coral larvae settlement, low sedimentation rates, oceanographic boundary conditions (e.g. salinity, temperature and density of the ocean water) and a sufficient supply of nutrients through topographically controlled currents systems (Mortensen et al., 2001; Roberts et al., 2003; Thiem et al., 2006; Dorschel et al., 2007; Dullo et al., 2008; Van Rooij et al., 2011; Hebbeln et al., 2016). Alternatively, the "hydraulic theory" ~~supports~~ suggests that CWC ecosystems may be directly fueled by fluid seepage, providing a source of e.g. sulfur compounds, nitrogen compounds, P, CO_2 and/or hydrocarbons (Hovland, 1990; Hovland and Thomsen, 1997; Hovland et al., 1998; 2012). This relationship is supported by the common co-occurrence of CWC-mounds and hydrocarbon-rich seeps around the world, for example at the Hikurangi Margin in New Zealand (Liebetrau et al., 2010), the Brazil margin (e.g. Gomes-Sumida et al., 2004), the Darwin Mounds in the northern Rockall Trough (Huvenne et al., 2009), the Kristin field on the Norwegian shelf (Hovland et al., 2012), the western Alborán Sea (Margreth et al., 2011), and the Gulf of Cádiz (e.g. Díaz-del-Río et al., 2003; Foubert et al., 2008). However, CWCs may also benefit rather indirectly from seepage. For instance, methane-derived authigenic carbonates (MDACs) formed through the microbially mediated anaerobic oxidation of methane (AOM; Suess & Whiticar, 1989; Hinrichs et al., 1999; Thiel et al., 1999; Boetius et al., 2000; Hinrichs & Boetius, 2002) potentially provide hard substrata for larval settlement (e.g. Díaz-del-Rio et al., 2003; Van Rooij et al., 2011; Magalhães et al. 2012; Le Bris et al., 2016; Rueda et al., 2016). In addition, larger hydrocarbon-rich seepage related structures such as mud volcanoes and carbonate mud mounds act as morphological barriers favoring turbulent water currents that deliver nutrients to the corals (Roberts et al., 2009; Wienberg et al., 2009; Margreth et al., 2011; Vandorpe et al., 2016).

In the Gulf of Cádiz, most CWC occurrences are "coral graveyards" with only a few living corals that are situated along the Iberian and Moroccan margins. These CWC systems are typically associated with diapiric ridges, steep fault-controlled escarpments, and mud volcanoes (MVs) such as the Faro MV, Hesperides MV, Mekness MV, and ~~MVs~~ mud volcanoes in the Pen Duick Mud Volcano Province (Foubert et al., 2008; Wienberg et al., 2009). ~~MVs~~ Mud volcanoes (and other conspicuous morphological structures in this region such as pockmarks) are formed through tectonically induced fluid flow (Pinheiro et al., 2003; Somoza et al., 2003; Medialdea et al., 2009; León et al., 2010; 2012). The fluid flow is promoted through ~~This is because due to the~~ of the high regional tectonic activity and high fluid contents of sediments in this area (mainly CH_4 and, to a lesser extent, H_2S, CO_2, and N_2:

Pinheiro et al., 2003; Hensen et al., 2007; Scholz et al., 2009; Smith et al., 2010; González et al., 2012). However, the exact influence of fluid flow on CWC growth in this region remains elusive.

This study aims at elucidating the ~~linkage between the present-day formation of MDACs and CWCs development~~impact of hydrocarbon-rich seepage on CWCs, by testing whether or not CWCs in our working area have a chemosynthetic lifestyle, as well as outdrawing further ecological benefits and drawbacks of seepage-related processes for CWCs. ~~are indeed non-chemosynthetic fauna or harbor in fact chemosynthetic symbionts which allow them consuming some of the reduced compounds in sites of active emission of under seafloor fluids.~~ We address our hypothesis by the combined analyses of high-resolution ROV underwater images, geophysical data (e.g. seabed topography, deep high-resolution multichannel seismic reflection data), and sample materials (water analysis, petrographic features, $\delta^{13}C$- and $\delta^{18}O$-signatures of carbonates, lipid biomarkers and environmental 16s rDNA sequences of the prokaryotic microbial community). We focus our study in ~~along~~ the ~~the~~ Pompeia Province (**Fig. 1**), which encompasses mud volcanoes as the currently active Al Gacel MV (León et al., 2012), diapiric coral ridges and mounds~~. We address this question by the combined analyses of high-resolution ROV underwater images, geophysical data (e.g. seabed topography, deep high-resolution multichannel seismic reflection data), and sample materials (petrographic features, $\delta^{13}C$- and $\delta^{18}O$ signatures of carbonates, lipid biomarkers and environmental 16s rDNA sequences of the prokaryotic microbial community)~~. Based on our findings, we propose an integrated model to explain the tempo-spatial and genetic relations between CWCs, chemosynthetic fauna and hydrocarbon-rich seepage in the study area.

2. Materials and Methods

This study is based on data and samples from the Pompeia Province that were collected during the Subvent-2 cruise in 2014 aboard the R/V Sarmiento de Gamboa (**Fig. 1**). In order to elucidate the tempo-spatial and genetic relations between CWCs, chemosynthetic fauna and hydrocarbon-rich seepage in this area, we explored geological features (mud volcanoes and coral ridges) by means of underwater imaging and geophysical data. ~~Based on these findings, we sampled different geological structures (mud volcanoes and coral ridges).~~ ROV dives were carried out at the~~in~~ Al Gacel MV (D10 and D11) and the Northern Pompeia Coral Ridge (D03). Subsequently, we conducted detailed analyses on selected samples from sites that were characterized by different types of seepage during sampling (**Table 1**). Samples from the Al Gacel MV include authigenic carbonates (D10-R3, D10-R7, D11-R8), pore-water from the sediment (via micro-cores; D10-C5, D10-C8, D11-C10), and water from above the seafloor (via Niskin bottles; D10-N12, D11-N9). Furthermore, a scleractinian coral fragment was recovered from the Northern Pompeia Coral Ridge (D03-B1). All samples were immediately stored at room temperature (petrographic analysis), 4 °C (water, sediments and pore-water analysis), −20 °C (stable isotopic analysis), or −80 °C (environmental DNA analysis).

~~All samples were~~ All samples were taken with a ROV arm and immediately stored at room temperature

Con formato: Color de fuente: Automático

Con formato: Color de fuente: Automático

Con formato: Fuente: Negrita

Con formato: Color de fuente: Automático

Con formato: Sin Resaltar

Con formato: Color de fuente: Automático

2.1. Geophysical survey

Seabed topography of the studied sites was mapped by using an Atlas Hydrosweep DS (15 kHz and 320 beams) multibeam echosounder (MBES). Simultaneously, ultra-high resolution sub-bottom profiles were acquired with an Atlas Parasound P-35 parametric chirp profiler (0.5 – 6 kHz). Deep high-resolution multichannel seismic

reflection data was obtained using an array of 7 SERCEL gi-guns (system composed of 250 + 150 + 110 + 45 cubic inches) with a total of 860 cubic inches. The obtained data were recorded with an active streamer (SIG®16.3x40.175; 150 m length with 3 sections of 40 hydrophones each). The shot interval was 6 seconds and the recording length 5 seconds two-way travel time (TWT). Data processing (filtering and stacking) was performed on board with Hot Shots software.

2.2. Video survey and analysis

A remotely operated vehicle (ROV-6000 Luso, operated by EMEPC) was used for photographic documentation (high definition digital camera, 1024x1024 pixel) and sampling. The ROV was further equipped with a STD/CTD-SD204 sensor (*in-situ* measurements of salinity, temperature, oxygen, conductivity, sound velocity and depth), HydroC™ sensors (*in-situ* measurements of CO_2 and CH_4), ~~and~~ Niskin bottles (CH_4 concentrations, pH and redox potential measurements)~~s (CH_4 concentrations)~~, and a ROV core sampler (up to 16 cm).

2.2.1. Seawater and pore-water analysis

Niskin water-samples and micro-cores covering the water/sediment interface were recovered from an active pockmark close to the summit of the Al Gacel MV (D10-N4, D10-C5, D10-C8; same site as carbonate-sample D10-R7) as well as directly from its summit (D11-N9, D11-C10). Redox potentials (ORP) and pH-values of the water contained in the Niskin bottles were measured on site with HANNA portable instruments (HI 9025). Pore-water from the micro-cores was immediately extracted by centrifuging 10 cm thick slices of the sediments. Upon extraction, the pore-water was filtered with syringe filters of cellulose acetate (0.2 µm pore), acidified with distilled nitric acid (HNO_3), and stored under 4 °C before further analysis. Major and trace elements were subsequently measured with an Agilent 7500c inductively coupled plasma mass spectrometer (ICP-MS). Method accuracy and precision was checked by external standards (MIV, EPA, NASC, CASS). The precision was better than 5 % RSD (residual standard deviation) and the accuracy better than 4%. Concentrations of S^{2-} were measured with a Hanch-Lange DR 2800 spectrophotometer (cuvette test kit LCK 653).

~~One Niskin water-sample (D10-N4) and two micro-cores (D10-C5 and D10-C8) were recovered from active pockmark close to the summit of the Al Gacel MV (as carbonate D10-R7). Likewise, one Niskin water-sample (D11-N9) and one micro-core (D11-C10) were recovered from the summit of the Al Gacel MV. Redox potential (ORP) and pH were measured on site from Niskin water-samples with HANNA portable instruments (HI 9025).~~

2.3. Petrographic analysis

General petrographic analysis was performed on thin sections (ca. 60 µm thickness) with a Zeiss SteREO Discovery.V8 stereomicroscope (transmitted- and reflected light) linked to an AxioCam MRc 5-megapixel camera. Additional detailed petrographic analysis of textural and mineralogical features was conducted on polished thin sections (ca. 30 µm thickness) using a DM2700P Leica Microscope coupled to a DFC550 digital camera. Carbonate textures have been classified following Dunham (1962) and Embry & Klovan (1971).

2.4. Stable isotope signature~~s~~ ($\delta^{13}C$, $\delta^{18}O$) of carbonates

Stable carbon and oxygen isotope measurements were conducted on ca. 0.7 mg carbonate powder obtained with a high precision drill (ø 0.8 mm). The analyses were performed with a Thermo Scientific Kiel IV carbonate device

Con formato: Subíndice
Con formato: Color de fuente: Automático
Con formato: Heading3_BG, Izquierda, Interlineado: sencillo

coupled to a Finnigan Delta Plus gas isotope mass spectrometer. Accuracy and reproducibility were checked through the replicate analysis of a standard (NBS19) and reproducibility was better than 0.1 ‰. Stable carbon and oxygen isotope values are expressed in the standard δ notation as per mill (‰) deviations relative to Vienna Pee Dee Belemnite (VPDB).

2.5. Lipid biomarker analysis

2.5.1. Sample preparation

All materials used were pre-combusted (500 °C for >3 h) and/or extensively rinsed with acetone prior to sample contact. A laboratory blank (pre-combusted sea sand) was prepared and analyzed in parallel to monitor laboratory contaminations.

The preparation and extraction of lipid biomarkers was conducted in orientation to descriptions in Birgel et al. (2006). Briefly, the samples were first carefully crushed with a hammer and internal parts were powdered with a pebble mill (Retsch MM 301, Haan, Germany). Hydrochloric acid (HCl; 10 %) was slowly poured on the powdered samples which were covered with dichloromethane (DCM)-cleaned water. After 24 h of reaction, the residues (pH 3 – 5) were repeatedly washed with water and then lyophilized.

3 g of each residue was saponified with potassium hydroxide (KOH; 6 %) in methanol (MeOH). The residues were then extracted with methanol (40 mL, 2x) and, upon treatment with HCl (10 %) to pH 1, in DCM (40 mL, 2x) by using ultra-sonification. The combined supernatants were partitioned in DCM vs. water (3x). The total organic extracts (TOEs) were dried with sodium sulfate ($NaSO_4$) and evaporated with a gentle stream of N_2 to reduce loss of low-boiling compounds (cf. Ahmed and George, 2004).

Fifty percent of each TOE was separated over a silica gel column (0.7 g Merck silica gel 60 conditioned with *n*-hexane; 1.5 cm i.d., 8 cm length) into (a) hydrocarbon (6 mL *n*-hexane), (b) alcohol (7 mL DCM/acetone, 9:1, v:v) and (c) carboxylic acid fractions (DCM/MeOH, 3:1, v:v). Only the hydrocarbons were subjected to gas chromatography–mass spectrometry (GC-MS).

2.5.2. Gas chromatography–mass spectrometry (GC-MS)

Lipid biomarker analyses of the hydrocarbon fraction were performed with a Thermo Scientific Trace 1310 GC coupled to a Thermo Scientific Quantum XLS Ultra MS. The GC was equipped with a capillary column (Phenomenex Zebron ZB-5MS, 30 m length, 250 µm inner diameter, 0.25 µm film thickness). Fractions were injected into a splitless injector and transferred to the column at 300 °C. The carrier gas was He at a flow rate of 1.5 mL min^{-1}. The GC oven temperature was ramped from 80°C (1 min) to 310 °C at 5 °C min^{-1} (held for 20 min). Electron ionization mass spectra were recorded in full scan mode at an electron energy of 70 eV with a mass range of m/z 50 – 600 and scan time of 0.42 s. Identification of individual compounds was based on comparison of mass spectra and GC retention times with published data and reference compounds.

2.5.3 Gas chromatography–combustion–isotope ratio mass spectrometer (GC-C-IRMS)

Compound specific $\delta^{13}C$ analyses were conducted with a Trace GC coupled to a Delta Plus IRMS via a combustion-interface (all Thermo Scientific). The combustion reactor contained CuO, Ni and Pt and was operated at 940°C. The GC was equipped with two serially linked capillary columns (Agilent DB-5 and DB-1; each 30 m length, 250 µm inner diameter, 0.25 µm film thickness). Fractions were injected into a splitless injector and

transferred to the GC column at 290°C. The carrier gas was He at a flow rate of 1.2 ml min^{-1}. The temperature program was identical to the one used for GC-MS (see above). CO_2 with known $\delta^{13}C$ value and a standard (IAEA600) were used for internal calibration. Instrument precision was checked using a mixture of *n*-alkanes with known isotopic composition. Standard deviations of duplicate sample measurements were generally better than 1.0 ‰. Carbon isotope ratios are expressed as $\delta^{13}C$ (‰) relative to VPDB.

~~Compound specific $\delta^{13}C$ analyses were conducted with a Trace GC coupled to a Delta Plus IRMS via a combustion-interface (all Thermo Scientific). The combustion reactor contained CuO, Ni and Pt and was operated at 940°C. The GC was equipped with two serially linked capillary columns (Agilent DB-5 and DB-1; each 30 m length, 250 µm inner diameter, 0.25 µm film thickness). Fractions were injected into a splitless injector and transferred to the GC column at 290°C. The carrier gas was He at a flow rate of 20 ml min^{-1}. The temperature program was identical to the one used for GC-MS (see above). CO_2 with known $\delta^{13}C$ value was used for internal calibration. Instrument precision was checked using a mixture of *n*-alkanes with known isotopic composition. Carbon isotope ratios are expressed as $\delta^{13}C$ (‰) relative to VPDB.~~

2.6. Amplicon sequencing of 16S rRNA genes

2.6.1. DNA extraction and 16S rRNA gene amplification

Environmental DNA analyses of microbial communities were performed on a carbonate sample with embedded corals from the base of the Al Gacel MV (D10-R3), a carbonate sample from an active pockmark close to the summit of the Al Gacel MV (D10-R7), and a necrotic fragment of a living *Madrepora oculata* recovered from the Northern Pompeia Coral Ridge (D03-B1). About 1 – 4 g of solid samples were first mashed with mortar and liquid nitrogen to fine powder. Three biological replicates were used per sample. Total DNA was isolated with a Power Soil DNA Extraction Kit (MO BIO Laboratories, Carlsbad, CA). All steps were performed according to the manufacturer's instructions.

Bacterial amplicons of the V3 – V4 region were generated with the primer set MiSeq_Bacteria_V3_forward primer (5'-TCGTCGGCAGCGTCAGATGTGTATAAGAGACAGCCTACGGGNGGCWGCAG-3') and MiSeq_Bacteria_V4_reverse primer (5'-GTCTCGTGGGCTCGGAGATGTGTATAAGAGACAGGACTACHVGGGTATCTAATCC-3'). Likewise, archaeal amplicons of the V3 – V4 region were generated with the primer set MiSeq_Archaea_V3_forward primer (5'-TCGTCGGCAGCGTCAGATGTGTATAAGAGACAG-GGTGBCAGCCGCCGCGGTAA-3') and MiSeq_Archaea_V4_reverse primer (5'-GTCTCGTGGGCTCGGAGATGTGTATAAGAGACAG-CCCGCCAATTYCTTTAAG-3'). 50 µl of the PCR reaction mixture for bacterial DNA amplification, contained 1 U Phusion high fidelity DNA polymerase (Biozym Scientific, Oldendorf, Germany), 5% DMSO, 0.2 mM of each primer, 200 µM dNTP, 0.15 µl of 25 mM $MgCl_2$, and 25 ng of isolated DNA. The PCR protocol for bacterial DNA amplification included (i) initial denaturation for 1 min at 98 °C, (ii) 25 cycles of 45 s at 98 °C, 45 s at 60 °C, and 30 s at 72 °C, and (iii) a final extension at 72 °C for 5 min. The PCR reaction mixture for archaeal DNA amplification was similarly prepared but contained instead 1 µl of 25 mM $MgCl_2$ and 50 ng of isolated DNA. The PCR protocol for archaeal DNA amplification included (i) initial denaturation for 1 min at 98 °C, (ii) 10 cycles of 45 s at 98 °C, 45 s at 63 °C, and 30 s at 72 °C, (iii) 15 cycles of 45 s at 98 °C, 45 s at 53 °C, and 30 s at 72 °C, and (iv) a final extension at 72 °C for 5 min.

PCR products were checked by agarose gel electrophoresis and purified using the GeneRead Size Selection Kit (QIAGEN GmbH, Hilden, Germany).

2.6.2. Data analysis and pipeline

Illumina PE sequencing of the amplicons and further process of the sequence data were performed in the Göttingen Genomics Laboratory (Göttingen, Germany). After Illumina MiSeq processing, sequences were analyzed as described in Egelkamp et al. (2017) with minor modifications. In brief, paired-end sequences were merged using PEAR v0.9.10 (Zhang et al., 2014), sequences with an average quality score below 20 and containing unresolved bases were removed with QIIME 1.9.1 (Caporaso et al., 2010). Non-clipped reverse and forward primer sequences were removed by employing cutadapt 1.15 (Martin, 2011). USEARCH version 9.2.64 was used following the UNOISE pipeline (Edgar, 2010). In detail, reads shorter than 380 bp were removed, dereplicated, and denoised with the UNOISE2 algorithm of USEARCH resulting in amplicon sequence variants (ASVs) (Callahan et al., 2017). Additionally, chimeric sequences were removed using UCHIME2 in reference mode against the SILVA SSU database release 132 (Yilmaz et al., 2014). Merged paired-end reads were mapped to chimera-free ASVs and an abundance table was created using USEARCH. Taxonomic classification of ASVs was performed with BLAST against the SILVA database 132. Extrinsic domain ASVs, chloroplasts, and unclassified ASVs were removed from the dataset. Sample comparisons were performed at same surveying effort, utilizing the lowest number of sequences by random subsampling (20,290 reads for bacteria, 13,900 reads for archaea).
The paired-end reads of the 16S rRNA gene sequencing were deposited in the National Center for Biotechnology Information (NCBI) in the Sequence Read Archive SRP156750.

3. Results

3.1. The Pompeia Province — geological settings

The Pompeia Province is situated in the Gulf of Cádiz offshore Morocco, within the so-called Middle Moroccan Field (Ivanov et al., 2000) at water-depths between 860 and 1000 m (**Fig. 1**). It ~~compromises~~ encompasses the active Al Gacel MV (**Fig. 1, C**), another mud volcano which is extinct (further referred as extinct MV) and two east-west elongated ridges (Northern Pompeia Coral Ridge and Southern Pompeia Coral Ridge). CWCs occur on all of these morphological features and ~~S~~scattered coral-mounds surround the ridges with a smooth relief (**Fig. 1, B**). ~~CWCs were observed on seismic profiles resting on all these morphological features.~~ Detailed geological profiles and 3D images of these features are shown in **Figs. 2** and **3**.
The Al Gacel MV is a cone-shape structure, 107 m high and 944 m wide, with its summit at 762 m depth and surrounded by a 11 m deep rimmed depression (León et al., 2012) (**Fig. 1, C**). It is directly adjacent to the Northern Pompeia Coral Ridge (**Fig. 2, A–B**), which extends ca. 4 km in westward direction (**Fig. 2, A–B**) and it is terminated by the Pompeia Escarpment (**Fig. 1, B; Fig. 2, C**). High resolution seismic profiles of the Pompeia Escarpment show CWC build-ups (R1 to R4) with steep lateral scarps of ca. 40 m height (**Fig. 2, C**). The Al Gacel~~is~~ MV is of sub-circular shape and exhibits a crater at its top (**Fig. 2, A–B**).
Ultra-high resolution sub-bottom seismic profile crossing the Pompeia Province from northwest (NW) to southeast (SE) (**Fig. 3, A**), shows (i) the Al Gacel MV surrounded by bottom-current deposits, (ii) an up to 130 m high CWC framework, growing on top the Southern Pompeia Coral Ridge, and (iii) semi-buried CWC mounds surrounding the ridge in areas of low relief. These CWC mounds locally form smooth, up to 25 – 30 m high ~~top-~~

~~rounded~~topographic reliefs that are exposed, but then taper downward below the seafloor (applying sound speeds of 1750 m/s in recent sediments). Additionally, a multichannel seismic profile following the same track but with higher penetration below the seafloor (**Fig. 3, B**) shows high amplitude reflections inside the Al Gacel cone and enhanced reflections at the top of the diapirs (yellow dotted-line in **Fig. 3, B**), pointing to the occurrence of gas (hydrocarbon)-charged sediments. It furthermore exhibits breaks in seismic continuity and diapiric structures at different depths below the Southern Pompeia Coral Ridge and the Al Gacel MV, evidencing the presence of a fault system (**Fig. 3, B**). These tectonic structures may promote the development of overpressure areas (OP in **Fig. 3, B**) and consequent upward fluid flow to the surface.

3.2. ROV observation and measurements

Submersible ROV surveys at the Al Gacel MV (**Fig. 1, C**) revealed the presence of dispersed pockmark depressions at the eastern (Dive 10, 790 m) and northern flanks (Dive 11, 760 – 825 m depth). These sites are characterized by focused but low intensity seafloor bubbling (e.g. **Fig. 4, B**; **Fig. 5, A**). Analysis of water samples revealed CH_4-concentration up to 171 nM during Dive 10 and up to 192 nM during Dive 11 (Sánchez-Guillamón et al., 2015).

~~-~~Pockmarks ~~were essentially formed~~are typically characterized~~–~~ by grey-olive mud breccia sediments and ~~characterized by deposits of~~ authigenic carbonates, appearing in the center and edges~~,~~. The authigenic carbonates are~~ together~~ commonly assocaited with typical methane-seep related organisms (e.g. sulfide-oxidizing bacterial mats, chemosynthetic bivalves, siboglinid tubeworms) (**Fig. 4, B–C**; **Fig. 5**). Communities of non-chemosynthetic organisms (e.g. sponges, corals) were also found at pockmarks (**Fig. 4, B–C**; **Fig. 5, C**), but were more abundant in places where no seepage was detected (**Fig. 4, A**).

Observations with the submersible ROV at the Northern Pompeia Coral Ridge and the extinct MV (Dive 03) revealed widespread and abundant occurrences of dead scleractinian-corals (mainly *Madrepora oculata* and *Lophelia pertusa*) currently colonized by few living non-chemosynthetic organisms (e.g. *Corallium tricolor*, other octocorals, sea urchins) (**Fig. 6, B–D**). Locally, grey-black colored patches of sulfide-oxidizing bacterial mats surrounded by dead chemosynthetic bivalves (*Lucinoma asapheus* and *Thysira vulcolutre*) were ~~detected~~ observed (**Fig. 6, A**). CH_4-seepage appeared to be less than at the Al Gacel MV, with concentrations of 80 – 83 nM.

Water parameters display homogenous values between the four sampling sites (10 °C temperature, ca. 52 – 55 % dissolved oxygen, ca. 31 Kg/m^3 density) (**Table ~~1~~2**). At depths of 7~~6~~90 m (D10-N4, same site as carbonate D10-R7~~1-N9~~) and 7~~9~~60 m (D11-N9~~D10-N4, same site as carbonate D10-R7~~), the pH of seawater was 7.8~~5~~8 and 7.8~~8~~5, respectively (**Table 3**). T~~and t~~he same seawater samples exhibited ORP values ~~were~~of 136~~257~~ mV (D10-N4) and ~~136~~257 mV (D11-N9) (**Table 3**)~~, respectively~~. Further analysis of these seawater samples revealed Fe^{2+} -concentration of 0.~~31~~57 and ~~0.57~~0.31 µM, while S^{2-} values were nearly absent (below detection limit~~<0.003 µM~~) (**Table 2**). ~~Additionally,~~ Fe^{2+} concentrations in pore-waters ranged between 0.94 – 1.27 µM (D10-C5), 2.70 – 1.74 µM (D10-C8), and 2.39 – 5.32 µM (D11-C10). S^{2-} concentrations in pore-waters were below detection limit (D10-C5), 50.23 µM (D10-C8), and 0.47 µM (D11-C10) ~~and S^{2-} concentrations of pore-water samples (D10-C5, D10-C8, D11-C10) present values ranging between 0.94 – 1.27 µM, 2.70 – 1.74, and 2.39 – 5.32 µM, respectively~~ (**Table ~~2~~3**).

3.3. Petrography and stable isotopes signatures of carbonates ($\delta^{18}O$, $\delta^{13}C$)

Con formato: Color de fuente: Automático
Con formato: Color de fuente: Automático
Con formato: Color de fuente: Automático
Con formato: Color de fuente: Automático
Con formato: Color de fuente: Automático
Con formato: Color de fuente: Automático
Con formato: Color de fuente: Automático
Con formato: Fuente: Negrita
Con formato: Color de fuente: Automático
Con formato: Color de fuente: Automático
Con formato: Color de fuente: Automático
Con formato: Color de fuente: Automático
Con formato: Color de fuente: Automático
Con formato: Color de fuente: Automático
Con formato: Color de fuente: Automático
Con formato: Fuente: Negrita
Con formato: Color de fuente: Automático
Con formato: Color de fuente: Automático
Con formato: Color de fuente: Automático
Con formato: Color de fuente: Automático
Con formato: Color de fuente: Automático
Con formato: Color de fuente: Automático
Con formato: Color de fuente: Automático
Con formato: Fuente: Negrita
Con formato: Color de fuente: Automático
Con formato: Superíndice
Con formato: Color de fuente: Automático
Con formato: Sin Resaltar
Con formato: Color de fuente: Automático
Con formato: Fuente: Negrita, Color de fuente: Automático
Con formato: Color de fuente: Automático
Con formato: Color de fuente: Rojo

Sample D10-R3 derives from a field of carbonates at the base of the Al Gacel MV which is inhabited by sponges and corals (**Fig. 4, A**). The sample is a framestone composed of deep water scleractinian corals (*Madrepora* and rare *Lophelia*) (**Fig. 7, A–B**). The corals are typically cemented by microbial automicrite (*sensu* Reitner et al. 1995) followed by multiple generations of aragonite. A matrix of dark allomicrite (*sensu* Reitner et al. 1995) with oxidized framboidal pyrites and remains of planktonic foraminifera is restricted to few bioerosional cavities (ca. 5%) in the skeletons of dead corals (**Fig. 8, A–B**). $\delta^{13}C$ signatures of the matrix and cements range from −26.68 to −18.38 ‰, while the embedded coral fragments exhibit $\delta^{13}C$ values between −5.58 and −2.09 ‰ (**Fig. 7, B; Table 2~~3~~4**). The $\delta^{18}O$ values generally range from +2.35 to +3.92 ‰ (**Fig. 9; Table 4~~3~~2**).

Sample D10-R7 was recovered from a pockmark on the eastern site of the Al Gacel MV that is virtually influenced by active seepage (**Fig. 3, C**). It consists of black carbonate and exhibits a strong hydrogen sulfide (H_2S) odor (**Fig. 5, B**; **Fig. 7, C–D**). The top of this sample was inhabited by living octocorals (**Fig. 5, C)**, while chemosymbiotic siboglinid worms were present on the lower surface (**Fig. 5, D**). The sample is characterized by a grey peloidal wackestone texture consisting of allomicrite with abundant planktonic foraminifers and few deep water miliolids. The sample furthermore exhibits some fractured areas which are partly filled by granular and small fibrous cement, probably consisting of Mg-calcite. Locally, light brownish crusts of microbial automicrite similar to ones in D10-R3 are present (see above). Framboidal pyrite is abundant and often arranged in aggregates (**Fig. 8, C–D**). The carbonate exhibits $\delta^{13}C$ values ranging from −28.77 to −21.13 ‰ and $\delta^{18}O$ values from +2.37 to +3.15 ‰ (**Fig. 9; Table 2~~3~~4**).

Sample D11-R8 comes from an area with meter-sized carbonate blocks at the summit of the Al Gacel MV and is mainly colonized by sponges and serpulid worms (**Fig. 4, D**). The sample generally exhibits a light grey mud- to wackestone texture consisting of allomicrite with few scleractinian-coral fragments and planktonic foraminifers (**Fig. 7, E–F**). The carbonate furthermore contains abundant quartz silt and, locally, pyrite enrichments. A further prominent feature are voids that are encircled by dark grey halos and exhibit brownish margins (due to enrichments of very small pyrite crystals and organic matter, respectively). $\delta^{13}C$ signatures of the matrix and cements range from −14.82 to −14.74 ‰, while embedded coral fragments exhibit $\delta^{13}C$ values of −4.91 to −2.99 ‰ (**Fig. 7, F; Table 4~~3~~2**). $\delta^{18}O$ values generally range from +1.49 to +5.60 ‰ (**Fig. 9; Table 2~~3~~4**).

Sample D03-B1 is a necrotic fragment of a living scleractinian coral (*Madrepora oculata*) recovered from the Northern Pompeia Coral Ridge (**Fig. 6, D**; **Fig. 7, G**). The coral-carbonate exhibits $\delta^{13}C$ values ranging from −8.08 to −1.39 ‰ and $\delta^{18}O$ values from −0.31 to +2.26 ‰ (**Fig. 9**; **Table 2~~3~~4**).

3.4. Lipid biomarkers and compound specific carbon isotope signatures

The hydrocarbon fractions of the carbonate recovered from the active pockmark (D10-R7) mainly consist of the irregular, tail-to-tail linked acyclic isoprenoids 2,6,11,15-tetramethylhexadecane (C_{20}; crocetane), 2,6,10,15,19-pentamethylicosane (C_{25}; PMI), as well as of several unsaturated homologues of these compounds (**Fig. 10**). Additionally, it contains the regular, head-to-tail linked acyclic isoprenoid pristane (C_{19}).

The hydrocarbon fraction of the carbonate recovered from the summit of the Al Gacel MV (D11-R8) is dominated by *n*-alkanes with chain-lengths ranging from C_{14} to C_{33} (maxima at *n*-C_{16} and, subordinated, at *n*-C_{20} and *n*-C_{31}) (**Fig. 10**). The sample further contains pristane, a mixture of crocetane and the head-to-tail linked acyclic isoprenoid phytane (C_{20}) (co-eluting), as well as traces of PMI.

In the carbonate from the active pockmark (D10-R7), crocetane and PMI exhibited strongly depleted $\delta^{13}C$ values (−101.2 ‰ and −102.9 ‰, respectively). In the carbonate from the summit of the volcano (D11-R8),

crocetane/phytane and PMI showed less depleted $\delta^{13}C$ values (−57.2 ‰ and −74.3 ‰, respectively). $\delta^{13}C$ values of *n*-alkanes in the carbonate D11-R8 (*n*-C_{17-22}) ranged between −30.8 ‰ and −33.0 ‰ (**Table 5**).~~The sample further contains pristane, crocetane, the head-to-tail linked acyclic isoprenoid phytane (C_{20}) and traces of PMI. Crocetane and PMI exhibited strongly depleted $\delta^{13}C$ values in the carbonate from the active pockmark (D10-R7) (−101.2 ‰ and −102.9 ‰, respectively), while they showed less depleted $\delta^{13}C$ values in the carbonate from the summit of the volcano (D11-R8) (−57.2 ‰ and −74.3 ‰, respectively). $\delta^{13}C$ values of *n*-alkanes in the carbonate D11-R8 (*n*-C_{17-22}) ranged between −30.8 ‰ and −33.0 ‰ (**Table 34**).~~

3.5. DNA inventories (MiSeq Illumina sequences)

Bacterial DNA ~~(**Fig. 11, A**)~~ from samples D10-R3 (authigenic carbonate, base of the Al Gacel MV) and D03-B1 (*Madrepora oculata* fragment, Northern Pompeia Coral Ridge) mainly derives from taxa that typically thrive in the water-column (e. g. Actinobacteria, Acidobacteria, Chloroflexi, Bacteroidetes, Woeseiaceae, Dadabacteria, Kaiserbacteria, Poribacteria, Planctomycetes, Gemmatimonadetes) (**Fig. 11, A**). The sample D10-R3 furthermore contains bacterial DNA of the nitrite-oxidizing bacteria *Nitrospira sp*., while the sample D03-B1 contains DNA of the bacterial taxa Verrucomicrobia, Enterobacteria, and *Nitrosococcus*. Noteworthy, one amplicon sequence variant (ASV_189) with low number of clustered sequences has been found in D03-B1, identified as a methanotrophic symbiont of *Bathymodiolus mauritanicus* (see Rodrigues et al., 2013).

Up to 50 % of bacterial DNA in sample D10-R7 (authigenic carbonate, top of the Al Gacel MV) derives from taxa that are commonly associated with fluid seepage and AOM, i.e. sulfide-oxidizing bacteria, sulfate-reducing bacteria (SRB) and methane-oxidizing bacteria. The most abundant are SRB taxa like SEEP-SRB1, SEEP-SRB2, *Desulfatiglans*, *Desulfobulbus* and *Desulfococcus*, which typically form consortia with ANME archaea.

Archaeal DNA (**Fig. 11, B**) from samples D10-R3 and D03-B1 mainly consist of *Cenarchaeum sp.*, which represents 70 – 90 %. *Candidatus Nitrosopumilus* is the second most abundant in both samples, representing 5 – 20 %. In contrast, around 90 % of archaeal DNA in D10-R7 is related to ANME-1 and ANME-2 groups, in good concordance with the relative abundances of SRB DNA.

Details of the number of reads per taxa are shown in the supplementary data, **Tables 1** and **2**.

4. Discussion

4.1. Evidence ~~of~~ for hydrocarbon-rich seepage affecting the Pompeia Province

Two-dimensional multichannel-seismic images show that the Pompeia Province is affected by fluid expulsion related to compressional diapiric ridges and thrust faults (**Fig. 3, B**), as it has been reported from other areas of the Gulf of Cádiz (Somoza et al., 2003; Van Rensbergen et al., 2005; Medialdea et al., 2009). There seem to be different types of fault-conduit systems that link the overpressure zones (OP) with the seafloor (**Fig. 3, B**), controlling both the type and rate of seepage (e.g. eruptive, focused, diffused or intermittent, the latter referred to as "dripping-like" in the following). ~~Dripping-like refers to intermittent bubbling fluids.~~ At the Al Gacel MV, conduits are for instance mainly linked to faults and a dense hydro-fracture network, allowing the migration of hydrocarbon-rich muds from the overpressure zone to the surface. During active episodes, eruptions lead to the formation of mud-breccia flows as observed in gravity cores (e.g. León et al., 2012). During rather dormant episodes, focused and dripping-like seepage predominates, forming pockmark features (**Fig. 4, B**).

Currently, the Al Gacel MV is affected by continuous and focused dripping-like seepages. These sites of active seepage are characterized by carbonates that are suspected to be methane-derived (e.g. sample D10-R7, **Fig. 4, B–C**). In-situ ROV-measurements and subsequent water sample analysis demonstrated high concentrations of CH_4 in fluids that were escaping upon removal of the carbonate D10-R7 from the active pockmark (171 nM; **Fig. 5, A**) (Sánchez-Guillamón et al., 2015). This association suggests a genetic relationship between hydrocarbon-rich seepage and the carbonate, as also ~~evidenced~~ reflected~~by~~ ~~the~~ low $\delta^{13}C$ ~~-values~~signatures of the carbonates analyzed herein (down to ca. −30 ‰, **Fig. 9; Table ~~2~~3**). Indeed, the grey peloidal texture of this sample resembles that of AOM-derived automicrites from the Black Sea that are related to micro-seepage of methane (cf. Reitner et al., 2005). The here observed isotopically depleted acyclic isoprenoids such as crocetane and PMI ($\delta^{13}C$ values between ca. −103 and −57‰; **Fig. 10; Table ~~3~~4**) are typical fingerprints of AOM-associated Archaea (Hinrichs et al., 1999; Thiel et al., 1999, 2001; Peckmann et al., 2001; Peckmann & Thiel, 2004), which is also in good accordance with the high abundance of DNA related to ANME. At the same time, elevated concentrations of S^{2-} and Fe^{2+} in pore-waters of D10-C8 micro-core (0.23 µM and 1.74 µM, respectively; **Table 2**), abundant framboidal pyrite (**Fig. 8, C–D**) and SRB-related DNA in the carbonate (**Fig. 11**) evidence microbial sulfate reduction in the environment. All these data clearly demonstrate that the carbonates have been formed via AOM, fueled by fluids from the underlying mud diapir. ~~Furthermore, soluble S^{2-} value of 0.23 µM and Fe value of 1.74 µM were measured in pore-water of shallow cores sampled in the same area (D10-C8; **Table 2**). These values are higher than the concentration measured in seawater (D10-N4; **Table 2**), indicating sulfide is being produced by the activity of AOM and also being consumed before it reaches the water column as well as the reduced iron. At the same time, abundant framboidal pyrite in the carbonate (**Fig. 8, C–D**) and SRB-related DNA (**Fig. 11**) evidences microbial sulfate reduction in the environment. All these data clearly demonstrate that the carbonates have been formed via AOM, fueled by fluids from the underlying mud diapir.~~

Other carbonate samples from the Al Gacel MV (i.e. D10-R3 and D11-R8) probably have also been formed due to AOM as they are ~~also~~ isotopically depleted as well ($\delta^{13}C$ values between ca. −25 and −15 ‰, **Fig. 9**, **Table ~~3~~2**). However, no active gas bubbling was observed during sampling, even though both samples still contain open voids which could form pathways for ~~a continuous migration of~~ fluids. ~~In fact, s~~Several characteristics of these voids (e.g. dark halos formed by pyrite, brownish margins due to organic matter enrichments) are very similar to those of methane-derived carbonate conduits (cf. Reitner et al., 2015). This could imply that the intensity of hydrocarbon-rich seepage and consequently AOM, may have fluctuated through time. This is in good accordance with the~~e~~ relatively low dominance of crocetane and PMI in ~~the~~a carbonate ~~D11-R8~~sampled from the summit of Al Gacel MV (D11-R8; **Fig. 10**~~, as well as their~~. The moderately depleted $\delta^{13}C$ values of crocetane/phytane and PMI in this sample (−57.2 ‰ and −74.3 ‰, respectively; **Table 4**) could be due to mixing effects and are thus also in agreement with varying intensities of AOM in the environment. The ~~moderately depleted $\delta^{13}C$ values (−57.2 ‰ and −74.3 ‰, respectively; **Table 4**), could be due to mixing effects and thus be in good accordance with varying intensities of AOM in the environment. Also, the~~ presence of only few AOM-related DNA sequences (**Fig. 11**) and partly oxidized pyrites in the carbonate D10-R3 from the base of the Al Gacel MV (**Fig. 8, A–B**) are well in line with this scenario.

There is no evidence for eruptive extrusions of muddy materials at the coral ridges. In the Southern Pompeia Coral Ridge (**Fig. 3**), diapirs appear to rather promote an upward migration of hydrocarbon-rich fluids in a divergent way throughout a more extensive seabed area. This results in a continuous and diffused seepage, which promotes the occurrence of AOM and the formation of MDACs at the base of the ridges, related to the sulphate-methane

Con formato: Resaltar
Con formato: Color de fuente: Automático, Resaltar
Con formato: Fuente: Negrita, Color de fuente: Automático, Resaltar
Con formato: Color de fuente: Automático, Resaltar
Con formato: Resaltar
Con formato: Color de fuente: Automático, Resaltar
Con formato: Resaltar
Con formato: Fuente: Negrita
Con formato: Fuente: Sin Negrita

transition zone (SMTZ) ~~related to the sulphate-methane transition zone (SMTZ)~~ (Boetius et al., 2000; Hinrichs and Boetius, 2002; González et al., 2012a). This is in good accordance with the detection of methane (80 – 83 nM) at the Northern Pompeia Coral Ridge and the presence of sulfide-oxidizing bacterial mats and shells of dead chemosynthetic bivalves at the western part of the ridge (**Fig. 6, A**). Likewise, the CWC Mounds Field surrounding the Southern Pompeia Coral Ridge (**Fig. 3**) is thoroughly characterized by micro-seeps, due to ascending fluids from OPs through low-angle faults. This type of focused seepage may promote formation of MDAC pavements in deeper layers of the sediments (**Fig. 3**), similar to coral ridges along the Pen Duick Escarpment (Wehrmann et al., 2011). The generation of MDAC-hotspots at sites of such seepage also explain the geometry of the downward tapering cones (**Fig. 3**).

4.2. Ecological meaning of hydrocarbon-rich seepage for CWCs

Our data suggests contemporaneous micro-seepage and CWC growth in the Pompeia Province (e.g. **Fig. 4, B**). This relationship has also been observed elsewhere, e.g. in the North Sea and off Mid Norway (Hovland, 1990; Hovland & Thomsen, 1997), and the Angola margin (Le Guilloux et al., 2009). Corals utilize HCO_3^- deriving from both the environment and the internal production of CO_2 for skeleton biomineralization (Swart, 1983; Zoccola et al., 2015; Nakamura et al., 2018). Hence, a potential utilization of methane as a carbon source should be reflected in the $\delta^{13}C$ signatures of their skeletons. However, scleractinian fragments recovered from the Al Gacel MV (embedded in carbonates D10-R3 and D11-R8, from the base and summit of the volcano, respectively) and the Northern Pompeia Coral Ridge (D03-B1, necrotic part of a living *Madrepora oculata*) displayed barely depleted $\delta^{13}C$ values (ca. −8 to −1 ‰; **Fig. 9**; **Table ~~2~~3**), close to the $\delta^{13}C$ of marine seawater (0 ± 3 ‰, e.g. Hoefs, 2015). These values do not support ~~Since it has been proposed that corals utilize HCO_3^- deriving from both the environment and the internal production of CO_2 for skeleton biomineralization (Swart, 1983; Zoccola et al., 2015; Nakamura et al., 2018), we expect $\delta^{13}C$ values in corals' carbonates to reflect whether or not they use methane as a carbon source. In our study, $\delta^{13}C$ values This doesdo not support~~ a significant uptake of methane-derived carbon by the CWCs and thus a direct trophic dependency as previously proposed (Hovland, 1990). ~~Nevertheless, future analysis on living coral-tissue would conclude our suspects.~~ Furthermore, the only DNA in sample D03-B1 that could be attributed to a potential methanotrophic endosymbiont (ASV_189: Rodrigues et al., 2013) occurred in minor amounts and most likely represents contamination from the environment or during sampling. ~~More likely,~~It appears therefore more likely that the CWCs feed on a mixture of phytoplankton, zooplankton and dissolved organic matter as previously proposed for ones in other regions (Kiriakoulakis et al., 2005; Duineveld et al., 2007; Becker et al., 2009; Liebetrau et al., 2010). This is in good accordance with the presence of DNA from various common archaeal and bacterial taxa (e.g. Acidobacteria, Actinobacteria, Candidatus *Nitrosopumilus, Cenarchaeum sp.*) and some potential members of the corals' holobiont (e.g. Enterobacteria, Verrucomicrobia, *Nitrosococcus sp.*) (Sorokin, 1995; Rädecker et al., 2015; Webster et al., 2016) in sample D03-B1 (**Fig. 11**). Taken together, there is no evidence that CWCs in the working area harbor microbial symbionts which potentially could utilize the hydrocarbon-rich fluids. However, future analyses on living coral-tissue will be important to verify this conclusion.~~More likely, the CWCs feed on a mixture of phytoplankton, zooplankton and dissolved organic matter as previously proposed for ones in other regions (Kiriakoulakis et al., 2005; Duineveld et al., 2007; Becker et al., 2009; Liebetrau et al., 2010). This is in good accordance with the presence of DNA from various common archaeal and bacterial taxa (e.g. Acidobacteria, Actinobacteria, Candidatus *Nitrosopumilus, Cenarchaeum sp.*) and some~~

Con formato: Sin Resaltar
Con formato: Sin Resaltar
Con formato: Subíndice
Con formato: Superíndice
Con formato: Subíndice

~~potential members of the corals' holobiont (e.g. Enterobacteria, Verrucomicrobia, *Nitrosococcus sp.*) (Sorokin, 1995; Rädecker et al., 2015; Webster et al., 2016) in sample D03-B1 (**Fig. 11**).~~

CWC development and hydrocarbon-rich seepage ~~are consequently~~appear to be rather linked *via* the formation of MDAC deposits, which provide the hard substrata needed for CWC larval settlement (e.g. Díaz-del-Rio et al., 2003; Van Rooij et al., 2011; Magalhães et al., 2012; Le Bris et al., 2016; Rueda et al., 2016). If too severe, however, fluid flow and associated metabolic processes can result in local conditions that are lethal to CWCs (see 4.3). Moreover, AOM fueled by fluid flow can also cause an entombment of the CWCs by MDACs (Wienberg et al., 2009, Wienberg & Titschack, 2015), as observed in D10-R3 and D11-R8 carbonates from the Al Gacel MV (**Figs. 7 and 9**; **Tab~~s.~~les ~~2~~3 and ~~3~~4**). It is therefore not surprising that large CWC systems in the Pompeia Province are always linked to structures that are affected by rather mild, non-eruptive seepage (i.e. the extinct MV, the coral ridges and the CWC Mound Fields: **Figs. 3 and 6**). The observation that these systems are in large parts "coral graveyards" (**Fig. 6, B–D**), similar to other areas in the Gulf of Cádiz (see Foubert et al., 2008; Wienberg et al., 2009), may be explained by a post-glacial decrease in current strength (Foubert et al., 2008). In the light of our findings, however, they could also have been negatively affected by periods of intensive seepage during higher tectonic activity. Future studies are important to test this hypothesis in greater detail.

4.3. Spatio-temporal co-existence of CWCs and chemosynthetic organisms — the buffer effect

As discussed above, MDAC deposits are ecologically beneficial for CWCs, as they serve~~d~~ as optimal substrata even when seepage is still present (e. g. Hovland, 1990; Hovland & Thomsen, 1997; Le Guilloux et al., 2009; this study). Severe hydrocarbon-rich seepage, however, is ecologically stressful for the corals. Particularly, fluid- and AOM-derived hydrogen sulfide is considered problematic because of its role in coral necrosis (Myers & Richardson, 2009; García et al., 2016) and carbonate dissolution effects (Wehrmann et al., 2011).

Hydrogen sulfides can efficiently be buffered through the reaction with Fe-(oxyhydro)-oxides or Fe^{2+} dissolved in pore waters, ultimately forming pyrite (Wehrmann et al., 2011). Fe-(oxyhydro)-oxides nodules have previously been observed in the Iberian and Moroccan margins (González et al., 2009; 2012b), but not in the Pompeia Province. Instead, sulfide-oxidizing bacteria living in symbiosis with invertebrates (e.g. siboglinid worms: Petersen & Dubilier, 2009) (**Fig. 5, D**) and thriving in mats (**Fig. 4, C**; **Fig. 6, A**) were particularly prominent along this region. These microbes may form a biological buffer by withdrawing reduced sulfur species through their metabolic activity. Likewise, the consumption of methane and sulfate by AOM-microorganisms at active sites also contribute to CWCs colonization of the carbonates by reducing environmental acidification (seawater pH was 7.85 in the active pockmark from the Al Gacel MV; see section 3.2).

We propose that this biological buffer provides a further ecological linkage between hydrocarbon-rich seepage and cold-water corals along the Pompeia Province ("buffer effect model": **Fig. 12**). This model explains the observed co-existence of non-chemosynthetic corals (e.g. on top of D10-R7 carbonate: **Fig. 5**) with AOM-microorganisms and chemosynthetic sulfide-oxidizing organisms at pockmark sites at the Al Gacel MV (**Fig. 12**, A). At the same time, it is in line with associations of sulfide-oxidizing bacterial mats, scleractinian corals, and other non-chemosynthetic octocorals at diapiric ridges and coral mounds in the Northern Pompeia Coral Ridge (**Fig. 12, B, C**). The impact and exact capacity of this biological buffer, however, remains elusive and must be evaluated in future studies.

Con formato: Inglés (Estados Unidos)

5. Conclusions

Cold-water coral occurrences in the Pompeia Province (Gulf of Cádiz) are typically linked to hydrocarbon-seep structures like mud volcanoes and diapirs. The irregular topography of these structures affects bottom water-currents which supply nutrients to the corals. A further ecological benefit is the seepage-fueled formation of authigenic carbonates, which provide ideal substrates for coral larvae settlement. Cold-water corals therefore take indirectly advantages of seepage-related conditions, instead of feeding from the seeped fluids, such as sulfide and methane. However, increased fluid seepage appears to be ecologically disadvantageous as evidenced by corals embedded in some of the carbonates. Consequently, cold-water coral growth in these habitats depends directly on seepage intensity and how these fluids are drained onto the seafloor (i.e. eruptive, focused, diffused or dripping-like). Cold-water coral growth appears to be furthermore supported by the microbial-mediated removal of seepage-related toxic substances (e. g., reduced sulfur species through sulfide-oxidizing bacteria) and shaping of environmental conditions (e. g., pH-buffering through AOM). This biological buffer is possibly crucial to keep conditions favorable for the growth of cold-water corals in the studied area, particularly in times of increased fluid seepage.

~~The presence of cold-water corals related to hydrocarbon-seep structures like mud volcanoes and diapirs, is partly due to the irregular topography affecting bottom water-currents, which supply nutrients to the corals. Likewise, their tight linkage to active hydrocarbon-rich seepage occurs by means of the production of methane-derived carbonates and how they provide the hard substrate cold-water corals need to develop. The discovery of methane-derived carbonates with embedded corals evidences the decline of coral colonization when the intensity of the fluid seepage increases or becomes more violent. Consequently, cold-water coral growth in these habitats depends directly on seepage intensity and how these fluids are drained onto the seafloor (i.e. eruptive, focused, diffused or dripping-like). Furthermore, cold-water corals rely on the microbial AOM-mediated sulfur and sulfide oxidation to reduce seeped fluids in the environment, since they are harmful for the corals. This biological buffer is possibly crucial to keep conditions favorable for the growth of cold-water corals in the studied area, particularly in times of increased fluid seepage.~~

Con formato: Resaltar

Author contribution

Blanca Rincón-Tomás, Dominik Schneider and Michael Hoppert carried out the microbial analysis. Jan-Peter Duda carried out the biomarker analysis. Luis Somoza and Teresa Medialdea processed seismic and bathymetric data. Pedro Madureira processed ROV data. Javier González and Joachim Reitner carried out the petrographic analysis. Esther Santofimia and Enrique López-Pamo carried out the pore-water and seawater analysis. Joachim Reitner carried out the stable isotopic analysis. Blanca Rincón-Tomás prepared the manuscript with contributions from all co-authors.

Competing interests

The authors declare that they have no conflict of interest.

Acknowledgments

The authors thank the captain and the crew on board the R/V Sarmiento de Gamboa, as well as the UTM (Unidad de Tecnología Marina), that have been essential for the success of this paper. Data obtained on board is collected in the SUBVENT-2 cruise, which can be found in the IGME archive. This work was supported by the Spanish project SUBVENT (CGL2012-39524-C02) and the project EXPLOSEA (CTM2016-75947) funded by the Spanish Ministry of Science, Innovation and Universities.

References

Ahmed, M. and George, S.C.: Changes in the molecular composition of crude oils during their preparation for GC and GC–MS analyses, Org. Geochem., 35, 137–155, doi:10.1016/j.orggeochem.2003.10.002, 2004.

Becker, E. L., Cordes, E. E., Macko, S. A., and Fisher, C. R.: Importance of seep primary production to *Lophelia pertusa* and associated fauna in the Gulf of Mexico, Deep-sea Res Pt I, 56(5), 786–800, doi:10.1016/j.dsr.2008.12.006, 2009.

Birgel, D., Thiel, V., Hinrichs, K. U., Elvert, M., Campbell, K. A., Reitner, J., Farmer, J. D., and Peckmann, J.: Lipid biomarker patterns of methane-seep microbialites from the Mesozoic convergent margin of California, Org. Geochem., 37(10), 1289–1302, doi:10.1016/j.orggeochem.2006.02.004, 2006.

Boetius, A., Ravenschlag, K., Schubert, C. J., Rickert, D., Widdel, F., Gieseke, A., Amann, R., Jørgensen, B. B., Witte, U., and Pfannkuche, O.: A marine microbial consortium apparently mediating anaerobic oxidation of methane, Nature, 407 (6804), 623–626, doi:10.1038/35036572, 2000.

Callahan, B., MacMurdie, P. J., and Holmes, S. O.: Exact sequence variants should replace optional taxonomic units in marker-gene data analysis, ISME J., 11, 2639–2643, doi:10.1038/ismej.2017.119, 2017.

Caporaso, J.G., Kuczynski, J., Stombaugh, J., Bittinger, K., Bushman, F.D., Costello, E.K., Fierer, N., González-Peña, A., Goodrich, J. K., Gordon, J. I., Huttley, G. A., Knights, D., Koenig, J. E., Lozupone, C. A., McDonald, D., Muegge, B. D., Pirrung, M., Reeder, J., Sevinsky, J. R., Turnbaugh, P. J., Walters, W. A., Widmann, J., Yatsunenko, T., Zaneveld, J., and Knight, R.: QIIME allows analysis of high-throughput community sequencing data, Nat. Methods, 7, 335–336, doi:10.1038/nmeth.f.303, 2010.

Cordes, E., Arnaud-Haond, S., Bergstad, O., da Costa Falcão, A. P., Freiwald, A., Roberts, J. M., and Bernal, P.: Cold water corals, in: The First Global Integrated Marine Assessment, World Ocean Assessment I, United Nations, Cambridge University Press, Cambridge, United Kingdom, 2016.

Díaz-del-Río, V., Somoza, L., Martínez-Frías, J., Mata, M. P., Delgado, A., Hernandez-Molina, F. J., …, Vázquez, J. T.: Vast fields of hydrocarbon-derived carbonate chimneys related to the accretionary wedge/olistostrome of the Gulf of Cádiz, Mar. Geol., 195, 177–200, doi:10.1016/S0025-3227(02)00687-4, 2003.

Dorschel, B., Hebbeln, D., Foubert, A., White, M., and Wheeler, A. J.: Hydrodynamics and cold-water coral facies distribution related to recent sedimentary processes at Galway Mound west of Ireland, Mar. Geol., 244, 184–195, doi:10.1016/j.margeo.2007.06.010, 2007.

Duineveld, G. C., Lavaleye, M. S., Bergman, M. J., De Stigter, H., and Mienis, F.: Trophic structure of a cold-water coral mound community (Rockall Bank, NE Atlantic) in relation to the near-bottom particle supply and current regime, B. Mar. Sci., 81 (3), 449–467, 2007.

576 Dullo, W. C., Flögel, S., and Rüggerberg, A.: Cold-water coral growth in relation to the hydrography of the Celtic
577 and Nordic European continental margin, Mar. Ecol. Prog. Ser., 371, 165–176, doi:10.3354/meps07623,
578 2008.
579 Dunham, R. J., 1962, Classification of carbonate rocks according to their depositional texture, in: Classification
580 of Carbonate Rocks, Ham, W. E. (Eds.), American Association of Petroleum Geologists Memoir 1, Tulsa,
581 OK, 108–121, 1962.
582 Edgar, R. C.: USEARCH. http://www.drive5.com/usearch. 2010.
583 Egelkamp, R., Schneider, D., Hertel, R., and, Daniel, R.: Nitrile-Degrading Bacteria Isolated from Compost, Front.
584 Environ. Sci., 5, doi: 10.3389/fenvs.2017.00056, 2017.
585 Embry III, A. F., and Klovan, J. E.: A late Devonian reef tract on northeastern Banks Island, NWT, B. Can. Petrol.
586 Geol., 19(4), 730–781, 1971.
587 Foubert, A., Depreiter, D., Beck, T., Maignien, L., Pannemans, B., Frank. N., Blamart, D., and Henriet, J.:
588 Carbonate mounds in a mud volcano province off north-west Morocco: key to processes and controls,
589 Mar. Geol., 248, 74–96, doi: 10.1016/j.margeo.2007.10.012, 2008.
590 Garcia, G. D., Santos, E. D. O., Sousa, G. V., Zingali, R. B., Thompson, C. C., and Thompson, F. L.:
591 Metaproteomics reveals metabolic transitions between healthy and diseased stony coral *Mussismilia*
592 *braziliensis*, Mol. Ecol., 25(18), 4632–4644, doi:10.1111/mec.13775, 2016.
593 Goedert, J. L., and Peckmann, J.: Corals from deep-water methane-seep deposits in Paleogene strata of Western
594 Oregon and Washington, U.S.A., in: Cold-water corals and Ecosystems, Freiwald, A., and Roberts, J. M.
595 (eds.), Springer-Verlag, Berlin Heidelberg, 27–40, 2005.
596 Gomes-Sumida, P.Y., Yoshinaga, M.Y., Saint-Pastous Madureira, L.A., and Hovland, M.: Seabed pockmarks
597 associated with deep water corals off SE Brazilian continental slope, Santos Basin, Mar. Geol., 207, 159–
598 167, doi:10.1016/j.margeo.2004.03.006, 2004.
599 González, F. J., Somoza, L., Lunar, R., Martínez-Frías, J., Martín Rubí, J. A., Torres, T., Ortiz, J. E., Díaz-del-
600 Río, V., Pinheiro, L. M., and Magalhães, V. H.: Hydrocarbon-derived ferromanganese nodules in
601 carbonate mud mounds from the Gulf of Cádiz: mud-breccia sediments and clasts as nucleation sites,
602 Mar. Geol., 261, 64–81, doi:10.1016/j.margeo.2008.11.005, 2009.
603 González, F. J., Somoza, L., León, R., Medialdea, T., de Torres, T., Ortiz, J. E., Martínez-Frías, J., and Merinero,
604 R.: Ferromanganese nodules and micro-hardgrounds associated with the Cádiz Contourite Channel (NE
605 Atlantic): Palaeoenvironmental records of fluid venting and bottom currents, Chem. Geol., 310–311, 56–
606 78, doi: 10.1016/j.chemgeo.2012.03.030, 2012a.
607 González, F. J., Somoza, L., Medialdea, T., León, R., Torres, T., Ortiz, J. E., and Martín-Rubí, J. A.: Discovery of
608 ferromanganese hydrocarbon-related nodules associated with the Meknes mud volcano (Western
609 Moroccan margin). European Geoscience Union 2012 (EGU2012). Viena (Austria). Geophys. Res. Abs.
610 vol. 14, EGU2012-12306, 2012b.
611 Hebbeln, D., Van Rooij, D., and Wienberg, C.: Good neighbours shaped by vigorous currents: cold-water coral
612 mounds and contourites in the North Atlantic, Mar. Geol, 378, 171–185,
613 doi:10.1016/j.margeo.2016.01.014, 2016.
614 Hensen, C., Nuzzo, M., Hornibrook, E., Pinheiro, L.M., Bock, B., Magalhães, V.H., and Brückmann, W.: Sources
615 of mud volcano fluids in the Gulf of Cádiz — indications for hydrothermal imprint, Geochim.
616 Cosmochim. Ac., 71 (5), 1232–1248, doi:10.1016/j.gca.2006.11.022, 2007.

617 Hinrichs, K. -U., and Boetius, A.: The anaerobic oxidation of methane: new insights in microbial ecology and
618 biogeochemistry, in: Ocean Margin Systems, Wefer, G., Billett, D., Hebbeln, D., Jørgensen, B.B.,
619 Schlueter, M., Van Weering, T. (Eds.), Springer-Verlag, Berlin, 457–477, 2002.
620 Hinrichs, K. -U., Hayes, J. M., Sylva, S. P., Brewer, P. G., and De Long, E. F.: Methane-consuming archaebacteria
621 in marine sediments, Nature, 398, 802–805, doi:10.1038/19751, 1999.
622 Hoefs, J.: Stable Isotope Geochemistry, Springer, Berlin, 2015.
623 Hovland, M.: Do carbonate reefs form due to fluid seepage?, Terra Nova, 2, 8–18, doi:10.1111/j.1365-
624 3121.1990.tb00031.x, 1990.
625 Hovland, M., Jensen, S., and Indreien, T.: Unit pockmarks associated with *Lophelia* coral reefs off mid-Norway:
626 more evidence of control by 'fertilizing' bottom currents, Geo-Mar. Lett., 32 (5–6), 545–554,
627 doi:10.1007/s00367-012-0284-0, 2012.
628 Hovland, M., Mortensen, P. B., Brattegard, T., Strass, P., and Rokoengen, K.: Ahermatypic coral banks off mid-
629 Norway: evidence for a link with seepage of light hydrocarbons, Palaios, 13, 189–200, doi:10.1043/0883-
630 1351(1998)013<0189:ACBOME>2.0.CO;2, 1998.
631 Hovland, M., and Thomsen, E.: Cold-water corals — are they hydrocarbon seep related?, Mar. Geol., 137, 159–
632 164, doi:10.1016/S0025-3227(96)00086-2, 1997.
633 Huvenne, V. A., Masson, D. G., and Wheeler, A. J.: Sediment dynamics of a sandy contourite: the sedimentary
634 context of the Darwin cold-water coral mounds, Northern Rockall Trough, Int. J. Earth Sci., 98 (4), 865–
635 884, doi: 10.1007/s00531-008-0312-5, 2009.
636 Ivanov, M. K., Akhmetzhanov, A. M., and Akhmanov, G. G.: Multidisciplinary study of geological processes on
637 the North East Atlantic and Western Mediterranean Margins, in: Ioc. Tech. S., 56, UNESCO, 2000.
638 Kiriakoulakis, K., Fisher, E., Wolff, G. A., Freiwald, A., Grehan, A., and Roberts, J. M.: Lipids and nitrogen
639 isotopes of two deep-water corals from the North-East Atlantic: initial results and implications for their
640 nutrition, in: Cold-Water Corals and Ecosystems, Freiwald, A., Roberts, J. M. (Eds.), Erlangen Earth
641 Conf., Springer, Germany, 715–729, 2005.
642 Le Bris, N., Arnaud-Haond, S., Beaulieu, S., Cordes, E. E., Hilario, A., Rogers, A., van de Gaever, S., and
643 Watanabe, H.: Hydrothermal Vents and Cold Seeps, in: The First Global Integrated Marine Assessment,
644 United Nations, Cambridge University Press, Cambridge, United Kingdom, 2016.
645 Le Guilloux, E., Olu, K., Bourillet, J. F., Savoye, B., Iglésias, S. P., and Sibuet, M.: First observations of deep-sea
646 coral reefs along the Angola margin, Deep-sea Res. Pt. II, 56, 2394–2403,
647 doi:10.1016/j.dsr2.2009.04.014, 2009.
648 Liebetrau, V., Eisenhauer, A., and Linke, P.: Cold seep carbonates and associated cold-water corals at the
649 Hikurangi Margin, New Zealand: new insights into fluid pathways, growth structures and geochronology,
650 Mar. Geol., 272, 307–318, doi:10.1016/j.margeo.2010.01.003, 2010.
651 León, R., Somoza, L., Medialdea, T., Vázquez, J. T., González, F. J., López-González, N., Casas, D., del Pilar
652 Mata, M., del Fernández-Puga, C., Giménez-Moreno, C. J., and Díaz-del-Río, V.: New discoveries of
653 mud volcanoes on the Moroccan Atlantic continental margin (Gulf of Cádiz): morpho-structural
654 characterization, Geo-Mar. Lett., 32, 473–488, doi:10.1007/s00367-012-0275-1, 2012.
655 Magalhães, V. H., Pinheiro, L. M., Ivanov, M. K., Kozlova, E., Blinova, V., Kolganova, J., Vasconcelos, C.,
656 McKenzie, J. A., Bernasconi, S. M., Kopf, A., Díaz-del-Río, V., González, F. J., and Somoza, L.:

Formation processes of methane-derived authigenic carbonates from the Gulf of Cádiz, Sediment. Geol., 243–244, 155–168, doi:10.1016/j.sedgeo.2011.10.013, 2012.

Margreth, S., Gennari, G., Rüggeberg, A., Comas, M. C., Pinheiro, L. M., and Spezzferri, S.: Growth and demise of cold-water coral ecosystems on mud volcanoes in the West Alboran Sea: The messages from planktonic and benthic foraminifera, Mar. Geol., 282, 26–39, doi:10.1016/j.margeo.2011.02.006, 2011.

Martin, M.: Cutadapt removes Adapter Sequences from High-Throughput Sequencing Reads, EMBnet.jounal, 10–12, doi: 10.14806/ej.17.1.200, 2011.

Medialdea, T., Somoza, L., Pinheiro, L. M., Fernández-Puga, M. C., Vázquez, J. T., León, R., Ivanov, M. K., Magalhães, V., Díaz-del-Río, V., and Vegas, R.: Tectonics and mud volcano development in the Gulf of Cádiz, Mar. Geol., 261, 48–63, doi:10.1016/j.margeo.2008.10.007, 2009.

Mortensen, P. B., Hovland, M. T., Fossa, J. H., and Furevik, D. M.: Distribution, abundance and size of *Lophelia pertusa* coral reefs in mid Norway in relation to seabed characteristics, J. Mar. Biol. Assoc. UK, 81, 581–597, doi:10.1017/S002531540100426X, 2001.

Myers, J.L., and Richardson, L.L.: Adaptation of cyanobacteria to the sulfide-rich microenvironment of black band disease of coral, FEMS Microbiol. Ecol., 67, 242–251, doi:10.1111/j.1574-6941.2008.00619.x, 2009.

Nakamura, T., Nadaoka, K., Watanabe, A., Yamamoto, T., Miyajima, T., and Blanco, A. C.: Reef-scale modeling of coral calcification responses to ocean acidification and sea-level rise, Coral Reefs, 37, 2018.

Peckmann, J., Reimer, A., Luth, U., Luth, C., Hansen, B.T., Heinicke, C., Hoefs, J., and Reitner, J.: Methane-derived carbonates and authigenic pyrite from the northwestern Black Sea, Mar. Geol., 177, 129–150, doi:10.1016/S0025-3227(01)00128-1, 2001.

Peckmann, J., and Thiel, V.: Carbon cycling at ancient methane–seeps, Chem. Geol., 205 (3), 443–467, doi:10.1016/j.chemgeo.2003.12.025, 2004.

Petersen, J. M., and Dubilier, N.: Methanotrophic symbioses in marine invertebrates, Env. Microbiol. Rep., 1(5), 319–335, doi:10.1111/j.1758-2229.2009.00081.x, 2009.

Pinheiro, L. M., Ivanov, M. K., Sautkin, A., Akhmanov, G., Magalhães, V. H., Volkonskaya, A., Monteiro, J. H., Somoza, L., Gardner, J., Hamouni, N., and Cunha, M. R.: Mud volcanism in the Gulf of Cádiz: results from the TTR-10 cruise, Mar. Geol., 195, 131–151, doi:10.1016/S0025-3227(02)00685-0, 2003.

Rädecker, N., Pogoreutz, C., Voolstra, C. R., Wiedenmann, J., and Wild, C.: Nitrogen cycling in corals: The key to understanding holobiont functioning?, Trends Microbiol., 23 (8), 490–497, doi:10.1016/j.tim.2015.03.008, 2015.

Reitner, J., Gauret, P., Marin, F., and Neuweiler, F.: Automicrites in a modern marine microbialite. Formation model via organic martices (Lizard Island, Great Barrier Reef, Australia), Bull.-Inst. Oceanogr. Monaco, 14, 237–263, 1995.

Reitner, J., Blumenberg, M., Walliser, E. -O., Schäfer, N., and Duda, J. -P.: Methane-derived carbonate conduits from the late Aptian of Salinac (Marne Bleues, Vocontian Basin, France): Petrology and biosignatures, Mar. Petrol. Geol., 66 (3), 641–652, doi:10.1016/j.marpetgeo.2015.05.029, 2015.

Reitner, J., Peckmann, J., Blumenberg, M., Michaelis, W., Reimer, A., and Thiel, V.: Concretionary methane-seep carbonates and associated microbial communities in Black Sea sediments, Palaeogeogr., Palaeoclimatol., Palaeocl., 227, 18–30, doi:10.1016/j.palaeo.2005.04.033, 2005.

Roberts, J. M., Long, D., Wilson, J. B., Mortensen, P. B., and Gage, J. D.: The cold-water coral *Lophelia pertusa* (Scleractinia) and enigmatic seabed mounds along the north-east Atlantic margin: are they related?, Mar. Pollut. Bull., 46, 7–20, doi:10.1016/S0025-326X(02)00259-X, 2003.

Roberts, J. M., Wheeler, A. J., and Freiwald, A.: Reefs of the deep: the biology and geology of cold-water coral ecosystems, Science, 312 (5773), 543–547, doi:10.1126/science.1119861, 2006.

Roberts, J. M., Wheeler, A., Freiwald, A., and Cairns, S. (Eds.): Cold-water corals: the biology and geology of deep-sea coral habitats, Cambridge University Press, Cambridge, United Kingdom, 2009.

Rodrigues, C. F., Cunha, M. R., Génio, L., and Duperron, S.: A complex picture of associations between two host mussels and symbiotic bacteria in the Northeast Atlantic, Naturwissenschaften, 100, 21–31, doi:10.1007/s00114-012-0985-2, 2013.

Rogers, A. D.: The Biology of *Lophelia pertusa* (Linnaeus 1758) and other Deep-Water Reef-Forming Corals and Impacts from Human Activities, Int. Rev. Hydrobiol., 84 (4), 315–406, doi:10.1002/iroh.199900032, 1999.

Rueda, J. L., González-García, E., Krutzky, C., López-Rodríguez, J., Bruque, G., López-González, N., Palomino, D., Sánchez, R. F., Vázquez, J. T., Fernández-Salas, L. M., and Díaz-del-Río, V.: From chemosynthetic-based communities to cold-water corals: Vulnerable deep-sea habitats of the Gulf of Cádiz, Mar. Biodiver., 46, 473–482, doi:10.1007/s12526-015-0366-0, 2016.

Sánchez-Guillamón, O., García, M. C., Moya-Ruiz, F., Vázquez, J. T., Palomino, D., Fernández-Puga, M. C., and Sierra, A.: A preliminary characterization of greenhouse gas (CH_4 and CO_2) emissions from Gulf of Cádiz mud volcanoes, VIII Symposium MIA15, 2015.

Somoza, L., Ercilla, G., Urgorri, V., León, R., Medialdea, T., Paredes, M., González, F. J., and Nombela, M. A.: Detection and mapping of cold-water coral mounds and living *Lophelia* reefs in the Galicia Bank, Atlantic NW Iberia margin, Mar. Geol., 349, 73–90, doi:10.1016/j.margeo.2013.12.017, 2014.

Somoza, L., León, R., Ivanov, M. Fernández-Puga, M. C., Gardner, J. M., Hernández-Molina, F. J., Pinheiro, L. M., Rodero, J., Lobato, A., Maestro, A., Vázquez, J. T., Medialdea, T., and Fernández-Salas, L. M.: Seabed morphology and hydrocarbon seepage in the Gulf of Cádiz mud volcano area: Acoustic imagery, multibeam and ultra-high resolution seismic data, Mar. Geol., 195, 153–176, doi:10.1016/S0025-3227(02)00686-2, 2003.

Sorokin, Y. I.: Coral reef ecology, Springer, Germany, 1995.

Suess, E, and Whiticar, M. J.: Methane-derived CO_2 in pore fluids expelled from the Oregon subduction zone, Palaeogeogr., Palaeoclimatol., Palaeocl., 71, 119–136, doi:10.1016/0031-0182(89)90033-3, 1989.

Swart, P. K.: Carbon and Oxygen Isotope Fractionation in ScleracUnian Corals: a Review, Earth-Sci. Rev., 19, 51–80, 1983.

Thiel, V., Peckmann, J., Seifert, R.,Wehrung, P., Reitner, J., and Michaelis, W.: Highly isotopically depleted isoprenoids: molecular markers for ancient methane venting, Geochim. Cosmochim. Ac., 63, 3959–3966, doi:10.1016/S0016-7037(99)00177-5, 1999.

Thiel, V., Peckmann, J., Richnow, H.-H., Luth, U., Reitner, J., and Michaelis, W.: Molecular signals for anaerobic methane oxidation in Black Sea seep carbonates and a microbial mat, Mar. Chem. 73, 97–112, doi:10.1016/S0304-4203(00)00099-2, 2001.

Thiem, Ø., Ravagnan, E., Fosså, J. H., and Berntsen, J.: Food supply mechanisms for cold- water corals along a continental shelf edge, J. Marine Syst., 26, 1481–1495, doi:10.1016/j.jmarsys.2005.12.004, 2006.

Vandorpe, T., Martins, I., Vitorino, J., Hebbeln, D., García-García, M., and Van Rooij, D.: Bottom currents and their influence on the sedimentation pattern in the El Arraiche mud volcano province, southern Gulf of Cádiz, Mar. Geol., 378, 114–126, doi:10.1016/j.margeo.2015.11.012, 2016.

Vandorpe, T., Wienberg, C., Hebbeln, D., Van den Berghe, M., Gaide, S., Wintersteller, P., and Van Rooij, D.: Multiple generations of buried cold-water coral mounds since the Early-Middle Pleistocene Transition in the Atlantic Moroccan Coral Province, southern Gulf of Cádiz, Palaeogeogr., Palaeoclimatol., Palaeocl., 485, 293–304, doi:10.1016/j.palaeo.2017.06.021, 2017.

Van Rensbergen, P., Depreiter, D., Pannemans, B., Moerkerke, G., Van Rooij, D., Marsset, B., Akhmanov, G., Blinova, V., Ivanov, M., Rachidi, M., Magalhães, V., Pinheiro, L., Cunha, M., and Henriet, J.P.: The Arraiche mud volcano field at the Moroccan Atlantic slope, Gulf of Cádiz, Mar. Geol., 219, 1–17, doi:10.1016/j.margeo.2005.04.007, 2005.

Van Rooij, D., Blamart, D., De Mol, L., Mienis, F., Pirlet, H., Whermann, L. M., …, Henriet, J. -P.: Cold-water coral mounds on the Pen Duick Escarpment, Gulf of Cádiz: The MiCROSYSTEMS project approach, Mar. Geol., 282, 102–117, doi:10.1016/j.margeo.2010.08.012, 2011.

Watling, L., France, S. C., Pante, E., and Simpson, A.: Biology of Deep-Water Octocorals, in: Advances in Marine Biology Volume 60, Lesser, M. (Eds.), Academic Press, London, United Kingdom, 41–122, 2011.

Webster, N. S., Negri, A. P., Botté, E. S., Laffy, P. W., Flores, F., Noonan, S., Schmidt, C., and Uthicke, S.: Host-associated coral reef microbes respond to the cumulative pressures of ocean warming and ocean acidification Sci. Rep.-UK, 6, doi:10.1038/srep19324, 2016.

Wheeler, A. J., Beyer, A., Freiwald, A., de Haas, H., Huvenne, V. A., Kozachenko, M., Olu-Le Roy, K., and Opderbecke, J.: Morphology and environment of cold-water coral carbonate mounds on the NW European margin, Int. J. Earth Sci., 96, 37–56, doi:10.1007/s00531-006-0130-6, 2007.

Wehrmann, L. M. Templer, S. P., Brunner, B., Bernasconi, S. M., Maignien, L., and Ferdelman, T. G.: The imprint of methane seepage on the geochemical record an early diagenetic processes in cold-water coral mounds on Pen Duick Escarpment, Gulf of Cádiz, Mar. Geol., 118–137, doi:10.1016/j.margeo.2010.08.005, 2011.

Wienberg, C., Hebbeln, D., Fink, H. G., Mienis, F., Dorschel, B., Vertino, A., López-Correa, M., and Freiwald, A.: Scleractinian cold-water corals in the Gulf of Cádiz—first clues about their spatial and temporal distribution, Deep-sea Res. Pt. I, 56 (10), 1873–1893, doi:10.1016/j.dsr.2009.05.016, 2009.

Wienberg, C., and Titschack, J.: Framework-forming scleractinian cold-water corals through space and time: a late Quaternary North Atlantic perspective, in: Marine Animal Forests: The Ecology of Benthic Biodiversity Hotspots, Rossi, S., Bramanti, L., Gori, A., and Orejas, C. (Eds.), Springer, Cham, Switzerland, 1–34, 2015.

Yilmaz, P., Parfrey, L.W., Yarza, P., Gerken, J., Pruese, E., Quast, C., Schweer, T., Peplies, J., Ludwig, W., and Glöckner, F. O.: The SILVA and 'All-species Living Tree Project (LTP)' taxonomic frameworks, Nucleic Acids Res., 42, D643–D648, doi:10.1093/nar/gkt1209, 2014.

Zhang, J., Kobert, K., Flouri, T., and Stamatakis, A.: PEAR: a fast and accurate Illumina Paired-End reAd merger, Bioinformatics, 30 (5), 614–620, doi:10.1093/bioinformatics/btt593, 2014.

Zoccola, D. Ganot, P., Bertucci, A., Caminit-Segonds, N., Techer, N., Voolstra, C. R., Aranda, M., Tambutté, E., Allemand, D., Casey, J. R., and Tambutté, S.: Bicarbonate transporters in corals point towards a key step in the evolution of cnidarian calcification, Sci. rep.-UK, 5, 2015.

Con formato: Sangría: Izquierda: 0 cm, Primera línea: 0 cm

Con formato: Espacio Después: 6 pto

Table 1. General description and characterization of recovered samples for this study in the Al Gacel MV and Northern Pompeia Province.

	Site description	Coordinates	Depth (m)	Type	Sample
Al Gacel MV	Base of volcano characterized by non-chemosynthetic fauna	35° 26.51' N -6° 58.22' W	850 – 890	Carbonate	D10-R3
	Active pockmark	35° 26.47' N -6° 58.27' W	790	Carbonate	D10-R7
				Water	D10-N4
					D10-C5
					D10-C8
	Summit with metric carbonate blocks	35° 26.48' N -6° 58.35' W	763	Carbonate	D11-R8
		35° 26.48' N -6° 58.37' W	760	Water	D11-N9
					D11-C10
Northern Pompeia Coral Ridge	Sulfide-oxidizing bacterial mats and shells of chemosynthetic bivalves	35° 26.77' N -6° 59.94' W	829	Necrotic fragment of a living *Madrepora oculata* coral	D03-B1

Con formato: Sangría: Izquierda: 0 cm, Primera línea: 0 cm
Con formato: Fuente: Negrita
Con formato: Fuente: Negrita
Con formato: Izquierda, Interlineado: sencillo
Tabla con formato
Con formato: Centrado, Interlineado: sencillo
Con formato: Centrado
Con formato: Centrado, Interlineado: sencillo
Con formato: Centrado, Interlineado: sencillo
Con formato: Centrado
Con formato: Centrado
Con formato: Centrado, Interlineado: sencillo
Con formato: Centrado, Interlineado: sencillo
Con formato: Centrado, Interlineado: sencillo
Con formato: Centrado
Con formato: Fuente: Negrita
Con formato: Centrado, Sangría: Izquierda: 0,2 cm, Derecha: 0,2 cm, Interlineado: sencillo
Con formato: Centrado
Con formato: Centrado, Interlineado: sencillo
Con formato: Centrado, Interlineado: sencillo
Con formato: Centrado
Con formato: Centrado
Con formato: Centrado, Interlineado: sencillo
Con formato: Centrado, Interlineado: sencillo
Con formato: Centrado, Interlineado: sencillo
Con formato: Centrado
Con formato: Fuente: Negrita
Con formato: Centrado, Sangría: Izquierda: 0,2 cm, Derecha: 0,2 cm, Interlineado: sencillo
Con formato: Centrado, Interlineado: sencillo
Con formato: Centrado, Interlineado: sencillo
Con formato: Centrado
Con formato: Centrado
Con formato: Centrado, Interlineado: sencillo
Con formato: Fuente: Cursiva

Table ~~1~~2. *In-situ* water variables measured during sampling with ROV sensors.

	D10-R3	D10-R7	D11-R8	D03-B1
~~Coordinates~~	~~35° 26.51' N -6° 58.22' W~~	~~35° 26.47' N -6° 58.27' W~~	~~35° 26.48' N -6° 58.35' W~~	~~35° 26.77' N -6° 59.94' W~~
Temperature (°C)	10.07	10.5	10.02	10.04 – 10.05
~~Depth (m)~~	~~850 – 890~~	~~791~~	~~763~~	~~829~~
Conductivity (mS/cm)	39.13 – 39.62	39.05 – 39.43	-	-
Salinity (ppt)	-	-	35.56 – 35.86	35.67 – 35.91
Saturation of dissolved oxygen (%)	53.64 – 54.69	54.02 – 54.35	51.95 – 53.92	52.46 – 56.22
Dissolved oxygen (mg/l)	4.81 – 4.90	4.85 – 4.88	4.66 – 4.84	4.71 – 5.09
Density (kg/m^3)	31.03 – 31.42	30.94 – 31.24	30.92 – 31.08	31.26 – 31.41

Table ~~1~~2. On site measurements of soluble Fe^{2+} and S^{2+} values from seawater and pore-water. Please note that samples D10-C5, D10-C8 and D10-N4 were taken from the same site as the authigenic carbonate D10-R7 (see **Fig. 2**). d.l. = detection limit.

Sample	Type	Fe^{2+} (µM)	S^{2+} (µM)	pH	ORP (mV)
D10-C5 (0 – 6 cm)	Pore-water	0.94	< d.l.	-	-
D10-C5 (6 –16 cm)		1.27	< d.l.	-	-

Con formato: Sangría: Izquierda: 0 cm, Primera línea: 0 cm

Con formato: Sangría: Izquierda: 0 cm, Primera línea: 0 cm

Tabla con formato

Con formato: Fuente: Sin Negrita, Sin Resaltar

Con formato: Fuente: Sin Negrita, Sin Resaltar

Con formato: Fuente: Sin Negrita

Con formato: Fuente: Negrita

Con formato: Fuente: Negrita

Con formato: Superíndice

Con formato: Superíndice

Con formato: Fuente: Negrita

Con formato: Fuente: Negrita

Con formato: Centrado, Interlineado: sencillo

Con formato: Superíndice

Con formato: Superíndice

Con formato: Fuente: Negrita

Con formato: Centrado, Interlineado: sencillo

Tabla con formato

Con formato: Fuente: Negrita

Con formato: Fuente: Negrita

Con formato: Fuente: 10 pto

Con formato: Centrado, Interlineado: sencillo

Con formato: Fuente: 10 pto

Con formato: Fuente: 10 pto

Con formato: Centrado, Interlineado: sencillo

Con formato: Fuente: 10 pto

Con formato: Centrado, Interlineado: sencillo

Con formato: Fuente: 10 pto

Con formato: Fuente: 10 pto

Con formato: Centrado, Interlineado: sencillo

D10-C8 (0 – 6 cm)		2.70	< d.l.	-	-
D10-C8 (6 –16 cm)		1.74	0.23	-	-
D10-N4	Sea-water	0.57	< d.l.	7.88	136
D11-C10 (0 – 5 cm)	Pore-water	2.39	< d.l.	-	-
D11-C10 (5 – 15 cm)		5.32	0.47	-	-
D11-N9	Seawater	0.31	< d.l.	7.85	257

Con formato: Fuente: 10 pto
Con formato: Fuente: 10 pto
Con formato: Centrado, Interlineado: sencillo
Con formato: Fuente: 10 pto
Con formato: Centrado, Interlineado: sencillo
Con formato: Fuente: 10 pto
Con formato: Centrado, Interlineado: sencillo
Con formato: Fuente: 10 pto
Con formato: Centrado, Interlineado: sencillo
Con formato: Centrado, Interlineado: sencillo
Con formato: Fuente: 10 pto
Con formato: Centrado, Interlineado: sencillo
Con formato: Fuente: 10 pto
Con formato: Fuente: 10 pto
Con formato: Fuente: 10 pto
Con formato: Centrado, Interlineado: sencillo
Con formato: Fuente: 10 pto
Con formato: Fuente: 10 pto
Con formato: Centrado, Interlineado: sencillo
Con formato: Centrado, Interlineado: sencillo
Con formato: Fuente: 10 pto
Con formato: Centrado, Interlineado: sencillo
Con formato: Fuente: 10 pto
Con formato: Centrado, Interlineado: sencillo
Con formato: Fuente: 10 pto
Con formato: Centrado, Interlineado: sencillo
Con formato: Fuente: 10 pto
Con formato: Fuente: 10 pto

Pompeia Coral Ridge.

Table 2~~3~~4. Stable carbon and oxygen isotopes ($\delta^{13}C$, $\delta^{18}O$) of samples from the Al Gacel MV and the Northern Pompeia Coral Ridge.

Location	Sample	Origin of the carbonate	Identification number in Fig. 7	$\delta^{18}O$ (‰)	$\delta^{13}C$ (‰)
Al Gacel MV	D10-R3	Coral skeleton	1	2.35	−5.58
		Authigenic carbonate	2	3.37	−20.07
			3	3.60	−26.68
			4	3.70	−20.79
			5	3.45	−22.43
			6	3.80	−20.70
		Coral skeleton	7	3.28	−2.23
		Authigenic carbonate	8	3.83	−25.16
			9	3.63	−25.29
			10	3.91	−18.38
			11	3.60	−24.18
			12	3.55	−25.34
			13	3.56	−25.15
		Coral skeleton	14	3.50	−2.09
		Authigenic carbonate	15	3.92	−21.89
	D10-R7	Authigenic carbonate	21	2.90	−26.36
			22	3.15	−28.77
			23	2.94	−22.91
			24	2.67	−21.13
			25	2.37	−24.70
			26	2.56	−23.60
	D11-R8	Coral skeleton	16	1.49	−4.91
			17	2.13	−2.99

Con formato: Fuente: Negrita

			18	1.74	−4.22
		Authigenic carbonate	19	5.60	−14.82
			20	5.55	−14.74
Northern Pompeia Coral Ridge	D03-B1	Coral skeleton	1.1	−0.38	−7.93
			1.2	−0.86	−7.77
			1.3	−0.51	−7.35
			1.5	1.15	−5.26
			1.4	−1.03	−8.08
			1.6	0.69	−5.96
			1.7	0.54	−6.42

Table 234. Continued

Location	Sample	Origin of the carbonate	Identification number in Fig. 7	$\delta^{18}O$ (‰)	$\delta^{13}C$ (‰)
Northern Pompeia Coral Ridge	D03-B1	Coral skeleton	3.1	1.59	−2.08
			3.2	−0.31	−6.27
			3.3	−0.89	−6.78
			3.4	−0.94	−6.73
			3.5	1.84	−2.21
			3.6	2.26	−1.39
			3.7	1.74	−2.87

Table 345. Stable carbon isotopic composition ($\delta^{13}C$) of selected lipid biomarkers (in **Figure 10**). (*) Please note that crocetane in D11-R8 coelutes with phytane. n.d. = not detected.

Compound	D10-R7 (‰)	D11-R8 (‰)
n-C_{17}	n.d.	–33.0
n-C_{18}	n.d.	–31.8
n-C_{19}	n.d.	–31.1
n-C_{20}	n.d.	–30.8
n-C_{21}	n.d.	–31.5
n-C_{22}	n.d.	–31.7
Crocetane*	–101.2	–57.2
PMI	–102.9	–74.3

Con formato: Fuente: Negrita

Con formato: Fuente: Negrita

904
905
906
907
908
909
910

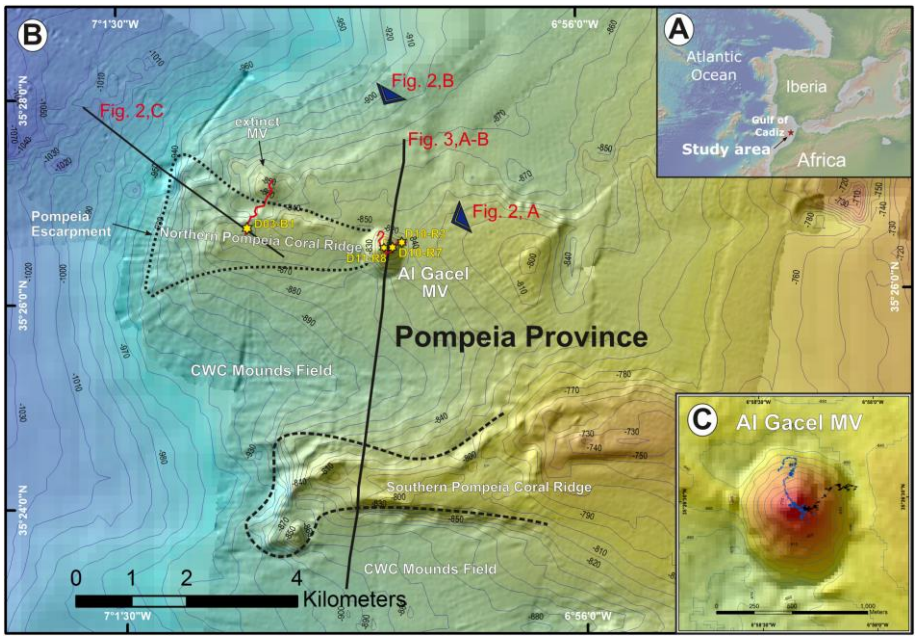

Figure 1. Bathymetric map of the study area. **A**: location of the Gulf of Cádiz between Spain, Portugal and Morocco. The study area is marked with a red star; **B**: the Pompeia Province including its different morphological features. Red lines indicate ROV-paths, yellow stars mark sampling sites; **C**: detailed map of the Al Gacel MV including pathways of Dive 10 and 11 (black and blue lines, respectively). Further details of the area are provided in **Figs. 2** and **3**.

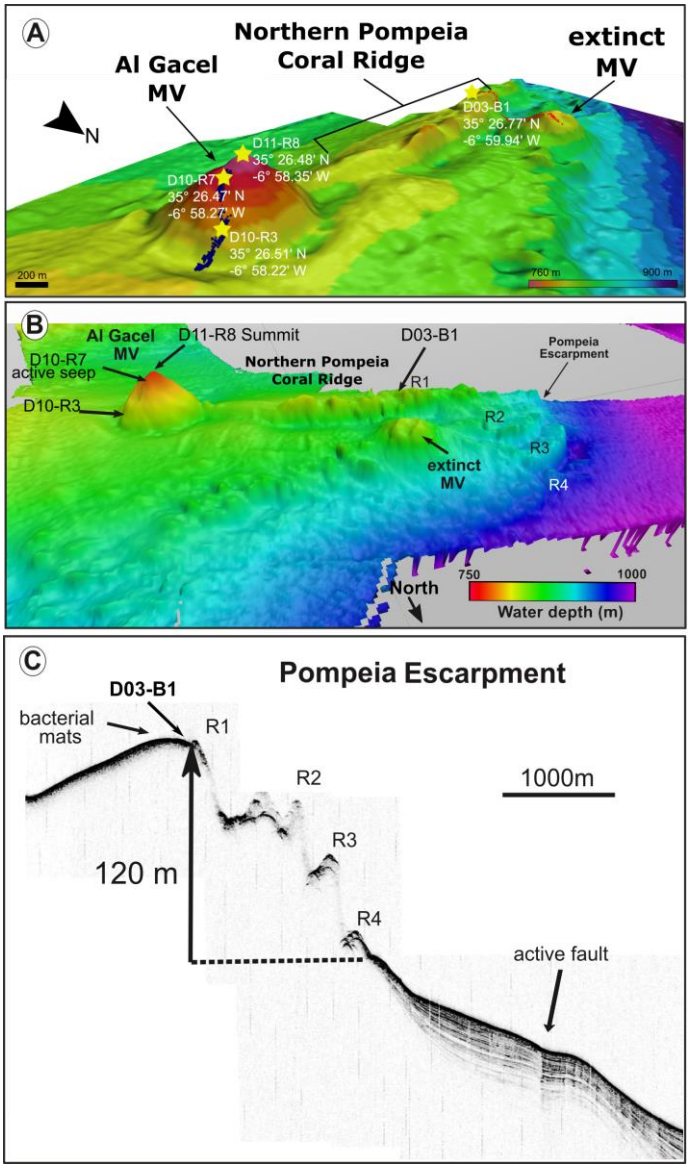

Figure 2. Bathymetric and seismic maps showing morphological features in northern Pompeia Province. **A–B**: bathymetric maps showing the Al Gacel MV, the Northern Pompeia Coral Ridge and the extinct MV. Yellow stars mark sampling sites. **C**: ultra-high seismic profile of the Pompeia Escarpment, westwards of the Northern Pompeia Coral Ridge.

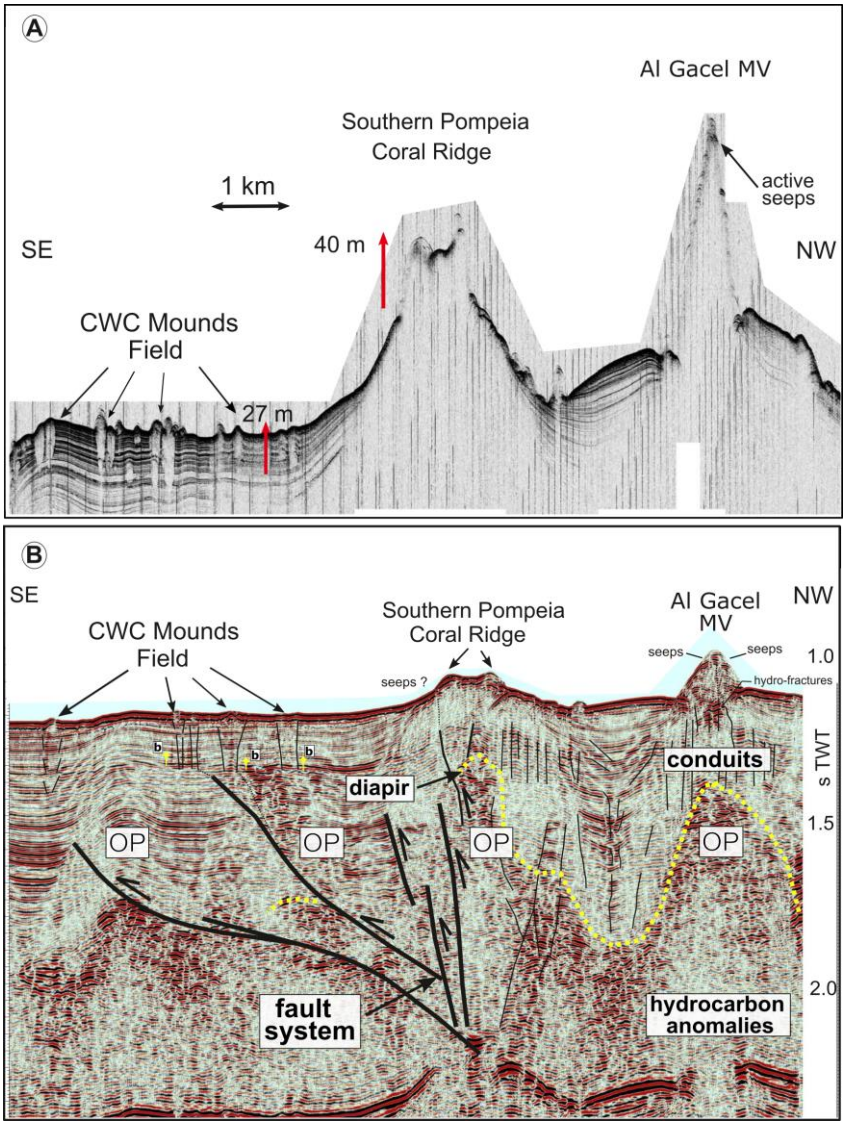

Figure 3. Ultra-high resolution (**A**) and multichannel (**B**) seismic profiles showing geological features in southern Pompeia Province. Note mud diapirism has been described in this area (Vandorpe et al., 2017). OP = overpressure zone.

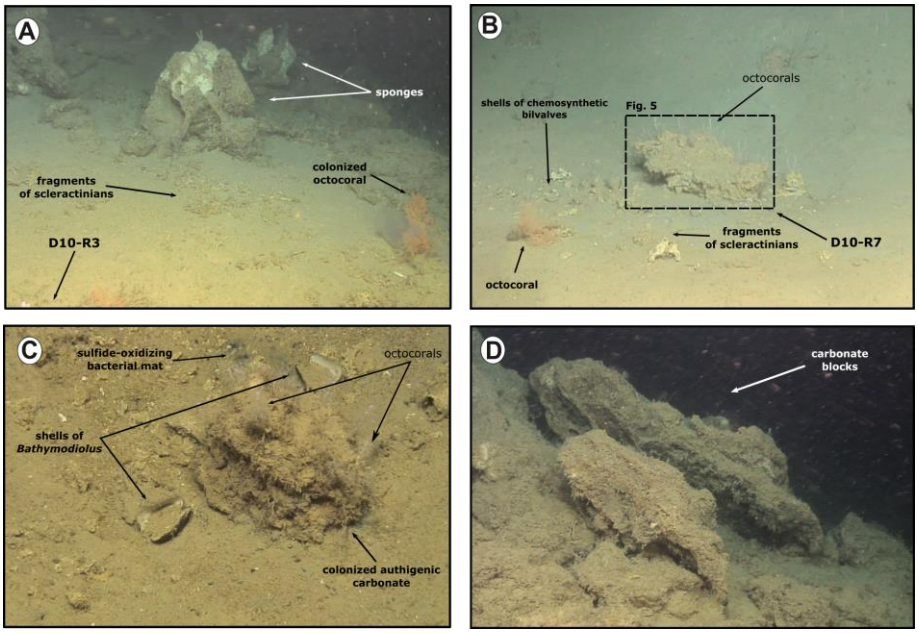

927
928 **Figure 4**: ROV still frames from the Al Gacel MV (Dives 10 and 11). **A**: eastern side of the volcano, displaying
929 a field of sponges, corals and carbonates; **B**–**C**: active pockmark sites on the east side of the volcano, displaying
930 authigenic carbonate surrounded by shells of chemosynthetic bivalves, fragments of scleractinian and octocorals,
931 as well as sulfide-oxidizing bacterial mats; **D**: metric-sized carbonate blocks located in a slope at the summit of
932 the volcano.
933
934

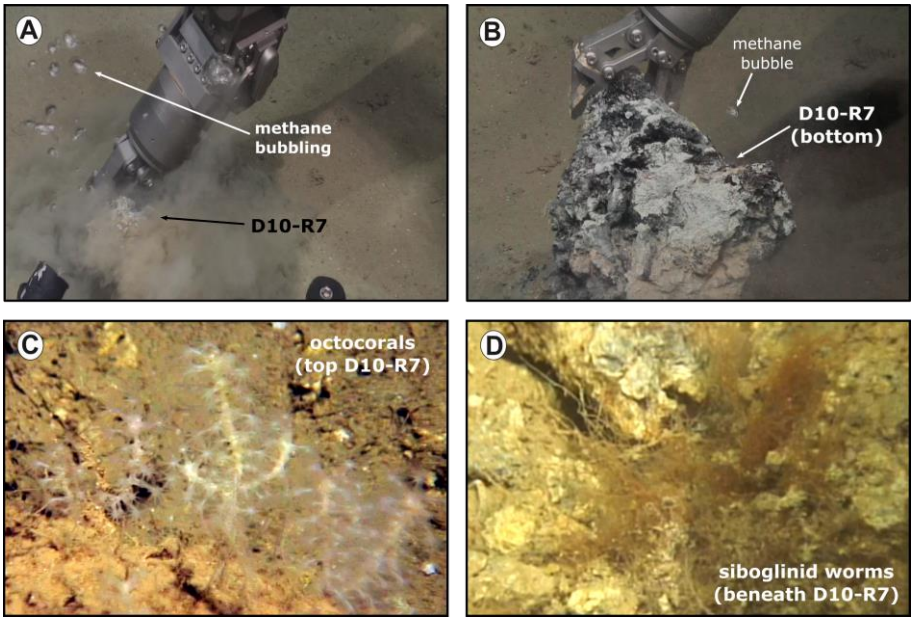

Figure 5. ROV still frames from the active pockmark site shown in **Fig. 4**, **B**. **A–B**: release of bubbles while sampling; **C**: detailed photograph of the octocorals on top of the carbonate; **D**: detailed still frame from siboglinid worms beneath the carbonate.

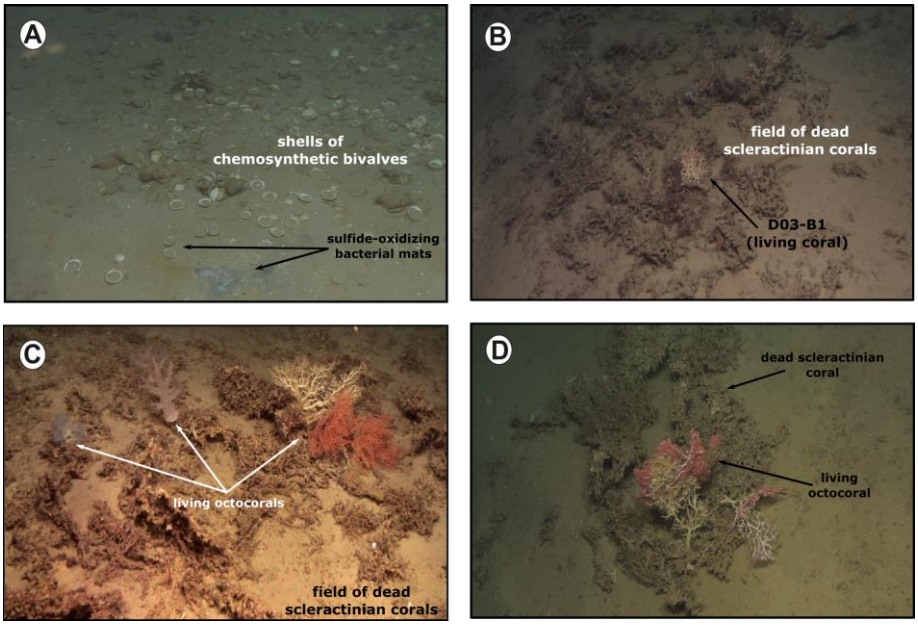

942
943 **Figure 6.** ROV still frames from the Northern Pompeia Coral Ridge and extinct MV (Dive 03), where there is
944 currently a diffused seepage of fluids. **A**: abundant shells of chemosynthetic bivalves with sulfide-oxidizing
945 bacterial mats at the western site of the Northern Pompeia Coral Ridge; **B**–**D**: field of dead scleractinian-corals
946 colonized by living corals; **D**: still frame from the extinct MV.
947

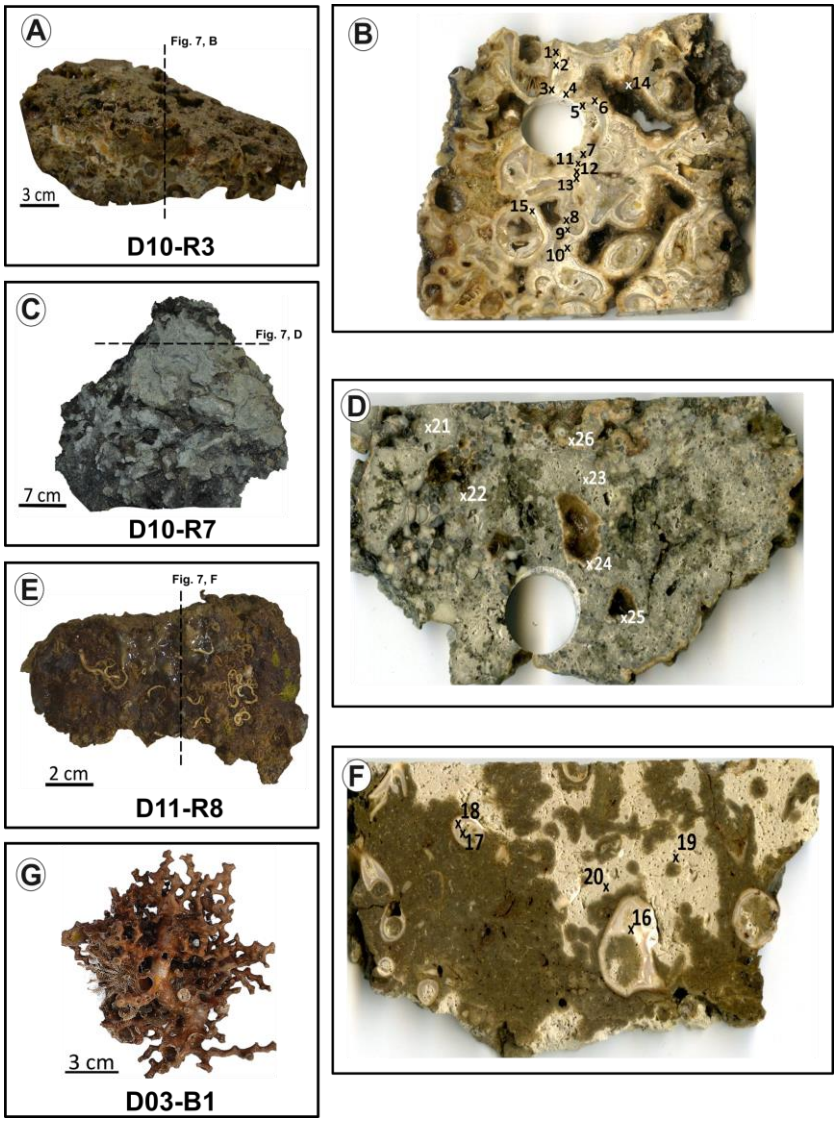

Figure 7. Photographs of analyzed samples including sampling sites for stable carbon and oxygen isotope ($\delta^{13}C$, $\delta^{18}O$) analysis (crosses with numbers). Values of the stable isotopic analyses are found in **Table 2**. **A–B**: D10-R3 carbonate with embedded corals; **C–D**: D10-R7 carbonate with strong H_2S odor; **E–F**: D11-R8 carbonate with embedded corals; **G**: D03-B1 scleractinian-coral fragment, *Madrepora oculata*. Please note that we cannot determine whether the corals were alive or dead the time they were buried by the carbonate.

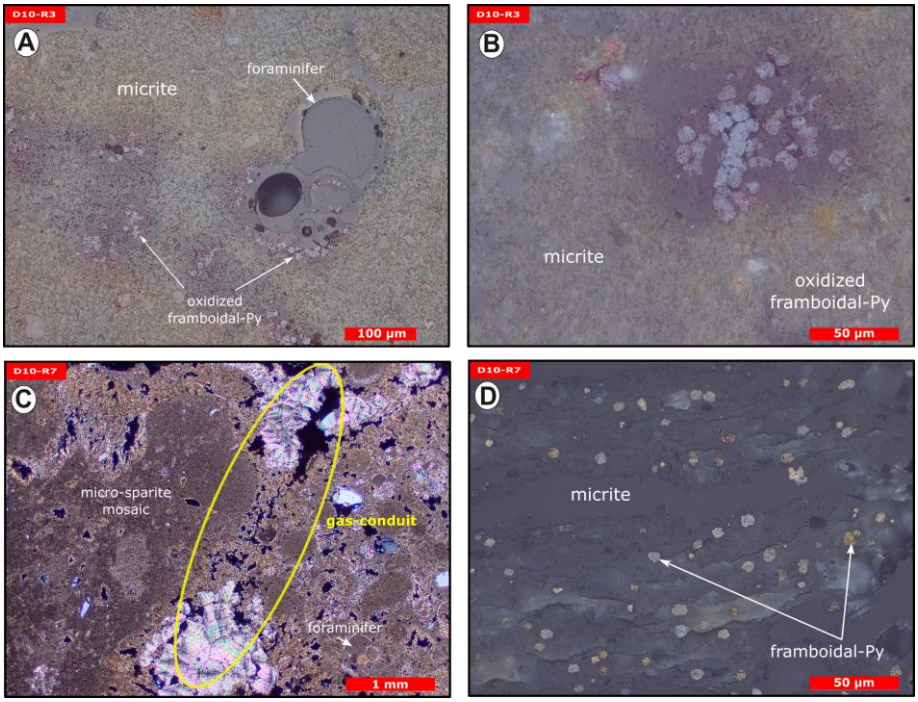

Figure 8. Thin section photographs of MDACs. **A–B**: D10-R3 consisting of a micritic matrix with scattered foraminifers and oxidized framboidal pyrites (reflected light); **C–D**: D10-R7 consisting of micritic and micro-sparitic carbonate with abundant unaltered framboidal pyrites (C, transmitted light; D, reflected light). Please note open voids which represent potential pathways for fluid seepage (yellow circle in C).

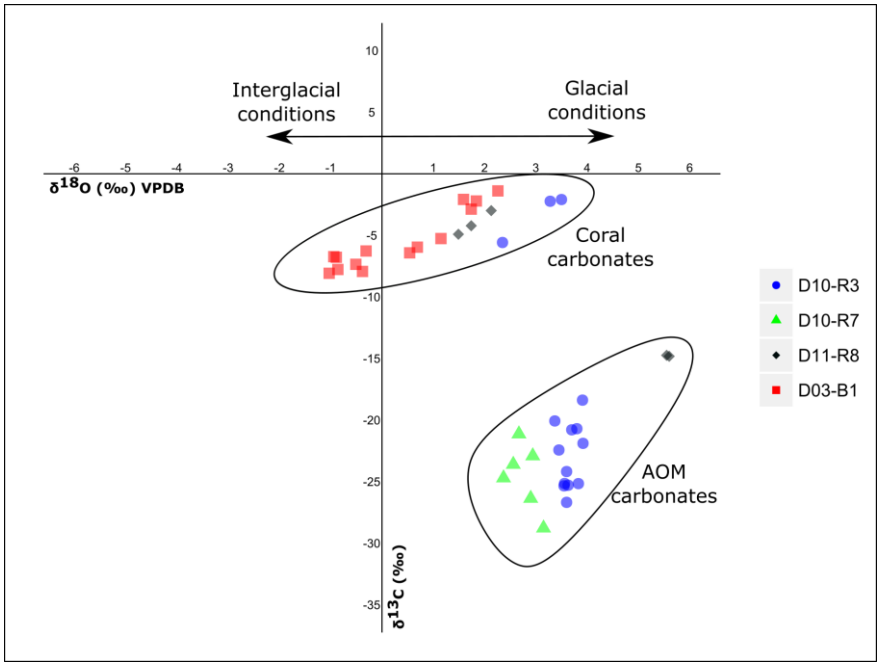

Figure 9. Stable carbon and oxygen isotopes ($\delta^{13}C$, $\delta^{18}O$) of samples from the Al Gacel MV and the Northern Pompeia Coral Ridge (see **Figure 3** for precise sampling points).

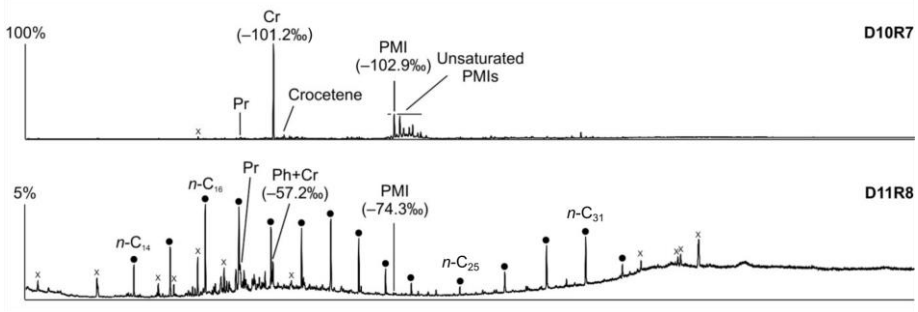

Figure 10. Total ion current (TIC) chromatograms of the analyzed samples. Isotopically depleted acyclic irregular isoprenoids such as Cr and PMI are typically found in settings influenced by the anaerobic oxidation of methane (AOM). Pr = pristane; Ph = phytane; Cr = crocetane; PMI = 2,6,10,15,19-pentamethylicosane; dots = n-alkanes; crosses = siloxanes (septum or column bleeding). Percentage values given on the vertical axes of chromatograms relate peak intensities to highest peak (Cr in D10-R7).

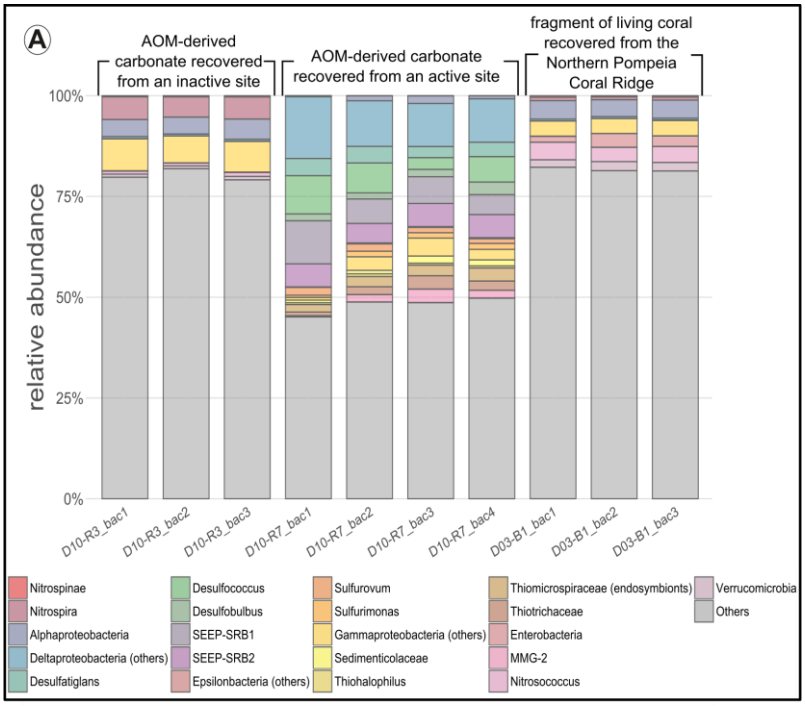
A
AOM-derived carbonate recovered from an inactive site
AOM-derived carbonate recovered from an active site
fragment of living coral recovered from the Northern Pompeia Coral Ridge
relative abundance
100%
75%
50%
25%
0%
D10-R3_bac1
D10-R3_bac2
D10-R3_bac3
D10-R7_bac1
D10-R7_bac2
D10-R7_bac3
D10-R7_bac4
D03-B1_bac1
D03-B1_bac2
D03-B1_bac3
Nitrospinae
Nitrospira
Alphaproteobacteria
Deltaproteobacteria (others)
Desulfatiglans
Desulfococcus
Desulfobulbus
SEEP-SRB1
SEEP-SRB2
Epsilonbacteria (others)
Sulfurovum
Sulfurimonas
Gammaproteobacteria (others)
Sedimenticolaceae
Thiohalophilus
Thiomicrospiraceae (endosymbionts)
Thiotrichaceae
Enterobacteria
MMG-2
Nitrosococcus
Verrucomicrobia
Others

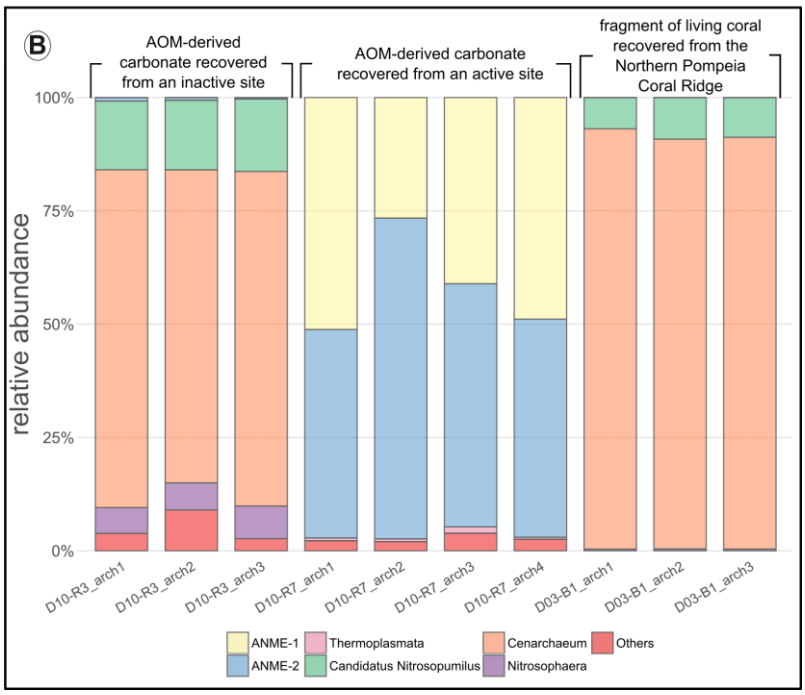
B
AOM-derived carbonate recovered from an inactive site
AOM-derived carbonate recovered from an active site
fragment of living coral recovered from the Northern Pompeia Coral Ridge
relative abundance
100%
75%
50%
25%
0%
D10-R3_arch1
D10-R3_arch2
D10-R3_arch3
D10-R7_arch1
D10-R7_arch2
D10-R7_arch3
D10-R7_arch4
D03-B1_arch1
D03-B1_arch2
D03-B1_arch3
ANME-1
ANME-2
Thermoplasmata
Candidatus Nitrosopumilus
Cenarchaeum
Nitrosophaera
Others

977

Figure 11. Bar chart representing relative abundances of prokaryotic taxa detected in each sample. **A**: bacterial taxa; **B**: archaeal taxa. In "others" aggrupation is included taxa related to ubiquitous organism normally found in sea- and seepage-related environments, and unclassified organisms. Number of reads per taxa detailed in **Table S1** (bacteria) and **Table S2** (archaea).

Con formato: Sangría: Izquierda: 0 cm, Primera línea: 0 cm

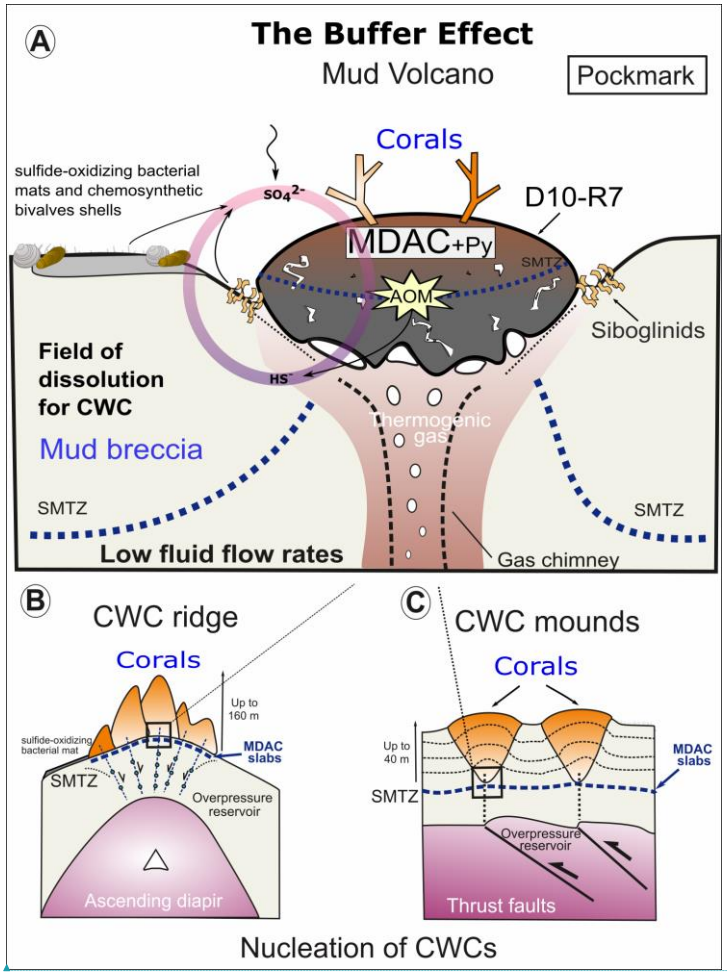

Con formato: Fuente: 10 pto

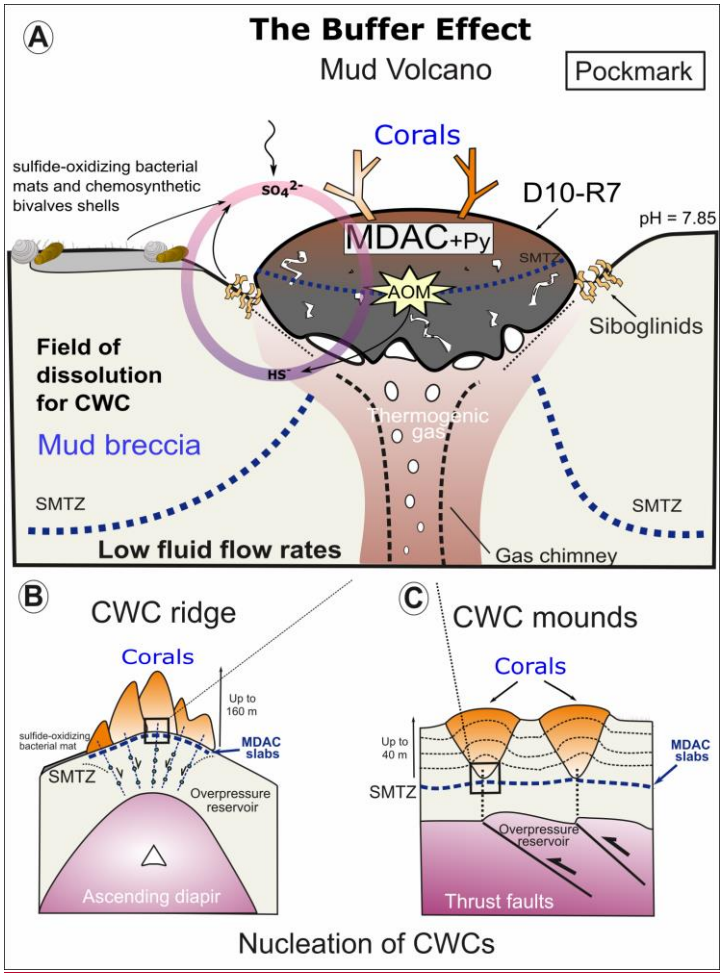

Figure 12. The buffer effect model. **A**: Buffer effect at pockmark sites (e.g. sampling site of D10-R7) where carbonates are formed directly on the bubbling site acting as a cap; **B**: Buffer effect at diapiric ridges where MDAC slabs are formed on the base of the ridge; **C**: Buffer effect at coral mounds where MDAC slabs are formed in deeper layers of the sediment. Py = pyrite, SMTZ: sulfur-methane transition zone.